RadioGraphics

From the Archives of the AFIP

Patterns of Contrast Enhancement in the Brain and Meninges[1]

CME FEATURE

See accompanying test at http://www.rsna.org/education/rg_cme.html

LEARNING OBJECTIVES FOR TEST 6

After reading this article and taking the test, the reader will be able to:

- Define contrast enhancement as it applies to CT and MR imaging of the brain and meninges.
- Explain the role of the blood-brain barrier and vascularity in contrast enhancement in the central nervous system.
- Use the patterns of enhancement to distinguish different pathologic processes in the brain and meninges.

TEACHING POINTS

See last page

James G. Smirniotopoulos, MD • Frances M. Murphy, MD, MPH
Elizabeth J. Rushing, MD • John H. Rees, MD • Jason W. Schroeder, LT, MC, USNR

Contrast material enhancement for cross-sectional imaging has been used since the mid 1970s for computed tomography and the mid 1980s for magnetic resonance imaging. Knowledge of the patterns and mechanisms of contrast enhancement facilitate radiologic differential diagnosis. Brain and spinal cord enhancement is related to both intravascular and extravascular contrast material. Extraaxial enhancing lesions include primary neoplasms (meningioma), granulomatous disease (sarcoid), and metastases (which often manifest as mass lesions). Linear pachymeningeal (dura-arachnoid) enhancement occurs after surgery and with spontaneous intracranial hypotension. Leptomeningeal (pia-arachnoid) enhancement is present in meningitis and meningoencephalitis. Superficial gyral enhancement is seen after reperfusion in cerebral ischemia, during the healing phase of cerebral infarction, and with encephalitis. Nodular subcortical lesions are typical for hematogenous dissemination and may be neoplastic (metastases) or infectious (septic emboli). Deeper lesions may form rings or affect the ventricular margins. Ring enhancement that is smooth and thin is typical of an organizing abscess, whereas thick irregular rings suggest a necrotic neoplasm. Some low-grade neoplasms are "fluid-secreting," and they may form heterogeneously enhancing lesions with an incomplete ring sign as well as the classic "cyst-with-nodule" morphology. Demyelinating lesions, including both classic multiple sclerosis and tumefactive demyelination, may also create an open ring or incomplete ring sign. Thick and irregular periventricular enhancement is typical for primary central nervous system lymphoma. Thin enhancement of the ventricular margin occurs with infectious ependymitis. Understanding the classic patterns of lesion enhancement—and the radiologic-pathologic mechanisms that produce them—can improve image assessment and differential diagnosis.

Abbreviations: CNS = central nervous system, H-E = hematoxylin-eosin, WHO = World Health Organization

RadioGraphics 2007; 27:525–551 • **Published online** 10.1148/rg.272065155 • **Content Code:** NR

[1]From the Departments of Radiology and Radiological Sciences (J.G.S., J.H.R.); Neurology (J.G.S., F.M.M.), Biomedical Informatics (J.G.S.), and Pathology (E.J.R.), Uniformed Services University, 4301 Jones Bridge Rd, Bethesda, MD 20813; Departments of Radiologic Pathology (J.G.S.) and Neuropathology and Ophthalmic Pathology (E.J.R.), Armed Forces Institute of Pathology, Washington, DC; Department of Veterans Affairs, Veterans Health Administration, Washington, DC (F.M.M.); Department of Radiology, Georgetown University Medical Center, Washington, DC (J.H.R.); and Department of Radiology, National Naval Medical Center, Bethesda, Md (J.W.S.). Received August 21, 2006; revision requested September 20 and received November 21; accepted December 5. All authors have no financial relationships to disclose. **Address correspondence to** J.G.S. (e-mail: *james-smirnio@usuhs.mil*).

Introduction

Enhancement with contrast material has been used for cross-sectional neuroimaging since the early days of computed tomography (CT). Initially, both urographic and angiographic iodine-based contrast agents (which had already been approved for parenteral injection) were used for contrast material–enhanced CT studies. These agents have largely been supplanted by low- and iso-osmolar contrast agents that have a lower frequency of side effects and a higher safety margin. Between 1988 and 2004, five gadolinium-based contrast agents were approved by the U.S. Food and Drug Administration for intravascular injection for contrast-enhanced magnetic resonance (MR) imaging. There are many tools for analyzing MR or CT images to produce a differential diagnosis. Contemporary imaging includes not only the acquisition of static anatomic images but also dynamic, physiologic, and chemical imaging—all of which can be used to focus a differential diagnosis. This article highlights the use of contrast material as one of these tools, with discussions of the appearance and location of the common patterns of lesion enhancement seen on MR and CT images.

Mechanisms of Contrast Material Enhancement

Teaching Point

Contrast material enhancement in the central nervous system (CNS) is a combination of two primary processes: intravascular (vascular) enhancement and interstitial (extravascular) enhancement (1,2). Intravascular enhancement may reflect neovascularity, vasodilatation or hyperemia, and shortened transit time or shunting. The brain, spinal cord, and nerves create a selectively permeable capillary membrane to protect themselves from plasma proteins and inflammatory cells: the blood-brain barrier. This barrier is primarily a result of endothelial cell specialization, but it requires a close relationship of the foot process of the perivascular astrocytes in the brain and spinal cord. The neural capillaries have a continuous basement membrane, narrow intercellular gaps, junctional complexes, and a paucity of pinocytotic vesicles. The semipermeable blood-brain barrier blocks lipophobic compounds and creates a unique interstitial fluid environment for the neural tissues. In contrast, lipophilic compounds (measured by octanol/water partition fraction), as well as certain chemicals that are actively transported, may cross the blood-brain barrier with ease. Certain cells that possess the correct surface marker proteins may pass unimpeded through the blood-brain barrier, whereas most other cells are excluded.

After a bolus injection of contrast material into a large peripheral vein, the blood level of the agent rises rapidly, creating a gradient across the capillary endothelial membrane, since the extravascular interstitial fluid does not have the compound. In regions with relatively free capillary permeability, the contrast agent will leak across the vessel wall and begin to accumulate in the perivascular interstitial fluid. In the brain, spinal cord, and proximal cranial and spinal nerves, the intact blood-brain barrier will prevent leakage of contrast material. Interstitial enhancement is related to alterations in the permeability of the blood-brain-barrier, whereas intravascular enhancement is proportional to increases in blood flow or blood volume. At CT, intravascular and interstitial enhancement may be seen simultaneously. When rapid dynamic CT images are obtained, as in CT angiography, most of the observed enhancement is intravascular. When CT imaging is delayed for 10–15 minutes after a bolus infusion, most of the observed enhancement is interstitial. At intermediate times, or with a continuous drip infusion of contrast material, enhancement is a composite variable mixture of both intravascular and interstitial compartments.

Several features of the MR imaging protocols alter the observations of contrast material enhancement. Most pulse sequences are subject to the "flow void phenomena," whereby rapidly flowing fluids have low signal intensity (3). As a result, vascular shunt lesions, such as vein of Galen malformation and arteriovenous malformation, appear dark on MR images. In addition, interstitial enhancement on MR images requires both free water protons and gadolinium. If a tissue is "dry" (ie, without water or free water), gadolinium enhancement will not be observed on routine T1-weighted MR images. For example, the skull and dura mater usually show vivid en-

hancement of the falx and tentorium on contrast-enhanced CT images, but they do not routinely demonstrate similar enhancement on MR images. Normal dura mater, which is extraaxial nonneural connective tissue, does not have a blood-brain barrier, but it lacks sufficient water to show the T1 shortening required for enhancement on MR images.

Various physiologic and pathologic conditions (which may either be unrelated or secondary to the primary lesions under investigation) produce abnormal contrast enhancement. New blood vessels (angiogenesis), active inflammation (infectious and noninfectious), cerebral ischemia, and pressure overload (ecclampsia and hypertension) are all associated with alterations in permeability of the blood-brain barrier. In addition, reactive hyperemia and neovascularity often have increased blood volume and blood flow (compared with that in normal brain tissue) and typically will show a shortened mean transit time. These features of abnormally increased capillary permeability and altered blood volume and flow result in abnormal contrast enhancement on static gadolinium-enhanced MR images, static iodine-enhanced CT scans, and conventional angiograms. Similarly, results of perfusion and flow studies will be abnormal, regardless of whether flow is measured at MR imaging, CT, or angiography. CT and MR imaging can help measure relative cerebral blood flow (rCBF), relative blood volume (rCBV), and mean transit time (MTT). Angiographic signs of rCBV include dilated veins, early opacification reflects rCBF, and early draining veins indicate a shortened MTT.

Extraaxial Enhancement

Extraaxial enhancement in the CNS may be classified as either pachymeningeal or leptomeningeal. The pachymeninges (thick meninges) are the dura mater, which comprises two fused membranes derived from the embryonic meninx primativa: the periosteum of the inner table of the skull and a meningeal layer. Pachymeningeal enhancement may be manifested up against the bone, or it may involve the dural reflections of the falx cerebri, tentorium cerebelli, falx cerebelli, and cavernous sinus. The leptomeninges (skinny meninges) are the pia and arachnoid. Leptomeningeal enhancement may occur on the surface of the brain or in the subarachnoid space. Because the normal, thin arachnoid membrane is attached to the inner surface of the dura mater, the pachymeningeal pattern of enhancement is also described as *dura-arachnoid enhancement*. In comparison, enhancement on the surface of the brain is called pial or *pia-arachnoid enhancement*. The enhancement follows along the pial surface of the brain and fills the subarachnoid spaces of the sulci and cisterns. This pattern is often referred to as leptomeningeal enhancement and is usually described as having a "gyriform" or "serpentine" appearance.

Pachymeningeal or Dura-Arachnoid Enhancement

The vessels within the dura mater do not produce a blood-brain barrier. Endogenous and exogenous compounds, such as serum albumin, fibrinogen, and hemosiderin, readily leak into (and out of) the normal dura mater. Normal dural enhancement is well seen on CT scans in the dural reflections of the falx cerebri, tentorium cerebelli, and falx cerebelli. However, enhancement of the dura mater against the cortical bone of the inner table of the skull is usually inconspicuous and not recognized because it appears "white on white." On T1-weighted MR images, the normal dura mater and inner table bone are uniformly hypointense. After the administration of gadolinium-based contrast material, the normal dura mater shows only thin, linear, and discontinuous enhancement (4).

Extraaxial pachymeningeal enhancement may arise from various benign or malignant processes, including transient postoperative changes, intracranial hypotension, neoplasms such as meningiomas, metastatic disease (from breast and prostate cancer), secondary CNS lymphoma, and granulomatous disease.

Postoperative meningeal enhancement occurs in a majority of patients and may be dura-arachnoid or pia-arachnoid (5). In patients who have not undergone surgery, other causes of this enhancement pattern should be considered. Although such enhancement has been reported after uncomplicated lumbar puncture, this observation is rare, occurring in less than 5% of patients (6).

Figure 1. Dura-arachnoid pachymeningeal enhancement. **(a)** Diagram illustrates dura-arachnoid enhancement, which occurs adjacent to the inner table of the skull; in the falx within the interhemispheric fissure; and also in the tentorium between the cerebellum, vermis, and occipital lobes. Pure dural enhancement, without pial or subarachnoid involvement, will not fill in the sulci or basilar cisterns. **(b)** Postoperative coronal gadolinium-enhanced T1-weighted MR image of a patient in whom a shunt catheter had been placed in the high right parietal region (arrow) demonstrates diffuse and relatively thin dura-arachnoid enhancement along the inner table of the skull and in the dural reflections of the falx and tentorium (arrowheads). There are bilateral subdural fluid collections, larger on the right (*).

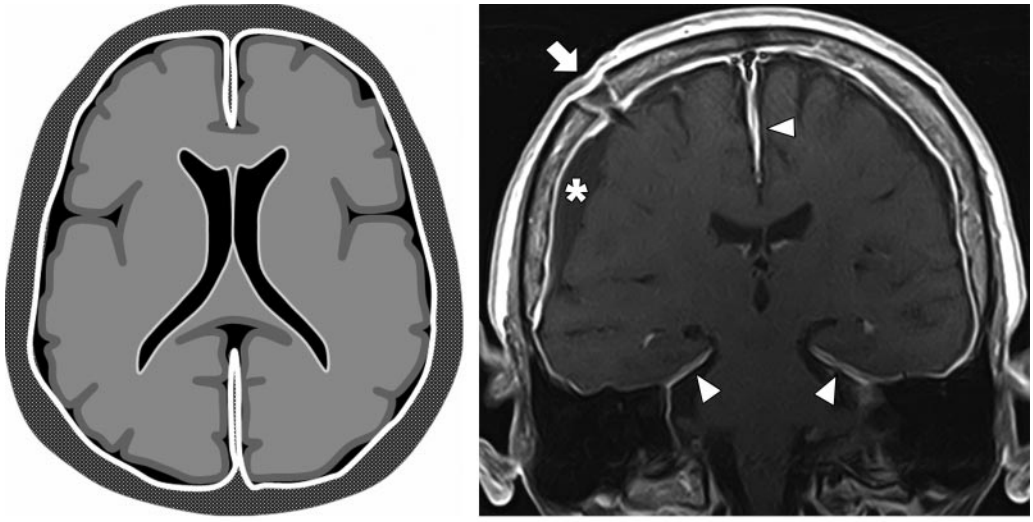

Teaching Point

Intracranial hypotension is a benign cause of pachymeningeal enhancement that may be localized or diffuse and can be seen on MR images in patients after surgery or with idiopathic loss of cerebrospinal fluid pressure (Figs 1, 2). When the cerebrospinal fluid pressure drops, there may be secondary fluid shifts that increase the volume of capacitance veins in the subarachnoid space. Prolonged intracranial hypotension may lead to vasocongestion and interstitial edema in the dura mater, findings similar to those seen in the dural tail of a meningioma. Intracranial hypotension may be caused by a skull fracture with leakage of cerebrospinal fluid. More often, it may follow an uncomplicated lumbar puncture; however, in many cases it is idiopathic. MR imaging is relatively sensitive and specific in the detection of benign or spontaneous intracranial hypotension. The classic findings and imaging features include headache that is orthostatic (postural) and worse when upright, thick linear enhancement of the pachymeninges, no enhancement of the sulci or brain surface, enhancement above and below the tentorium, enlargement of the pituitary gland, descent of the brain (low cerebellar tonsils, downward displacement of the iter of the third ventricle below the incisural line), and subdural effusions or hemorrhage in some patients (4,7,8).

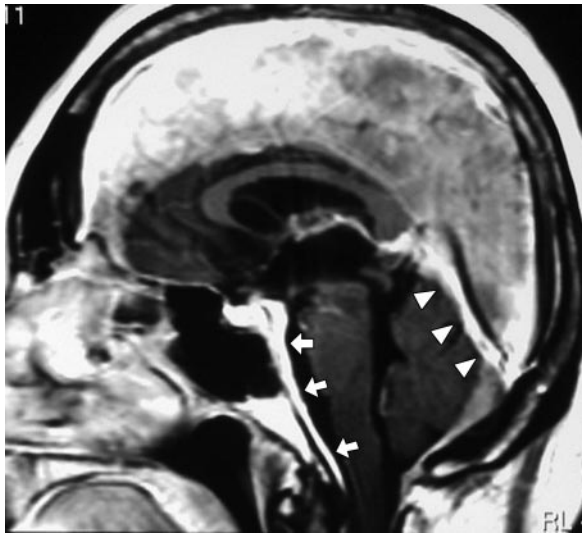

Figure 2. Dura-arachnoid pachymeningeal enhancement in a patient with intracranial hypotension. Sagittal gadolinium-enhanced T1-weighted MR image shows diffuse enhancement of the dura-arachnoid including the falx cerebri. Intracranial hypotension causes not only enhancement but also diffuse thickening of the pachymeninges. This abnormal thickening is especially prominent in the dura mater along the clivus (arrows) and tentorium (arrowheads). (Courtesy of Lazslo Mechtler, MD, Dent Neurological Institute, Buffalo, NY.)

Figures 3, 4. Dural tail enhancement with meningioma. **(3a)** Diagram illustrates the thin, relatively curvilinear enhancement that extends from the edge of a meningioma. Most of this enhancement is caused by vasocongestion and edema, rather than neoplastic infiltration. The bulk of the neoplastic tissue is in the hemispheric extraaxial mass; nonetheless, the dural tail must be carefully evaluated at surgery to avoid leaving neoplastic tissue behind. **(3b)** Gross photograph of a resected meningioma shows the dense, "meaty," well-vascularized neoplastic tissue. At the margin of the lesion, there is a "claw" of neoplastic tissue (arrowhead) overlying the dura mater (arrows) that is not directly involved with tumor. **(4)** Sagittal gadolinium-enhanced T1-weighted MR image reveals a large extraaxial enhancing mass. The dural tail (arrows) extends several centimeters from the smooth edge of the densely enhancing hemispheric mass. Most of this dural tail enhancement is caused by reactive changes in the dura mater.

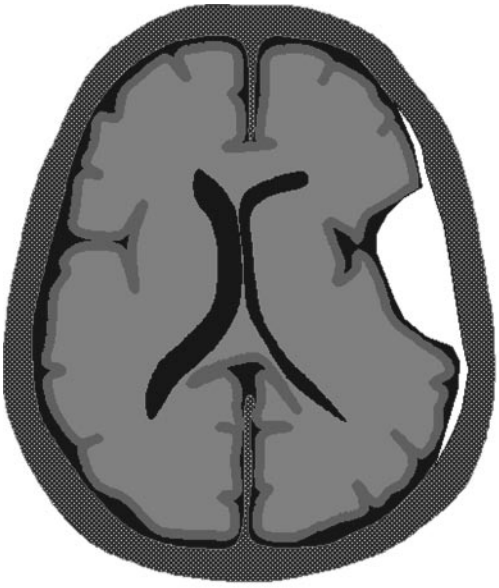

3a.

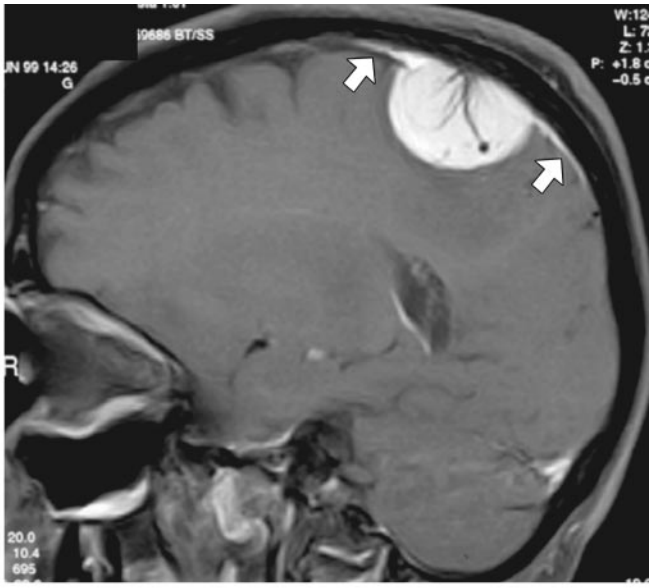

4.

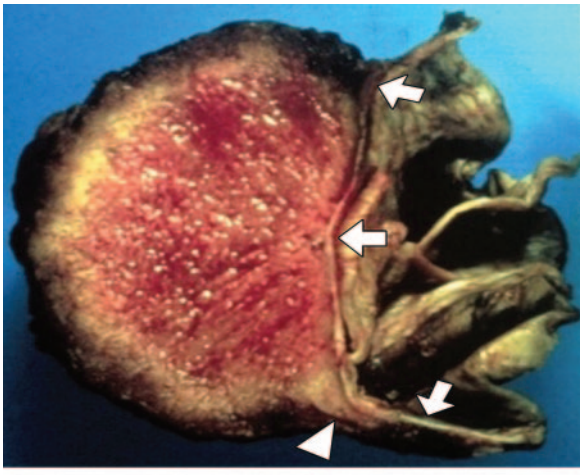

3b.

Pia-arachnoid (leptomeningeal) enhancement is not typical of benign intracranial hypotension, but it may be seen in postoperative patients.

Extraaxial neoplasms may produce pachymeningeal enhancement. The most common primary dural neoplasm is meningioma, a benign tumor of meningothelial cells (Figs 3, 4). Meningiomas are slowly growing, well-localized, WHO (World Health Organization) grade 1 lesions that are usually resectable for cure (9–11). They typically manifest in patients in the 4th–6th decades of life, and they are roughly twice as common in women as in men. The typical meningioma is a localized lesion with a broad base of dural attachment (Fig 3b). This neoplasm actually arises from the arachnoid membrane that is attached to the inner layer of the dura mater. Even in the early days of CT, the accuracy of cross-sectional imaging in the

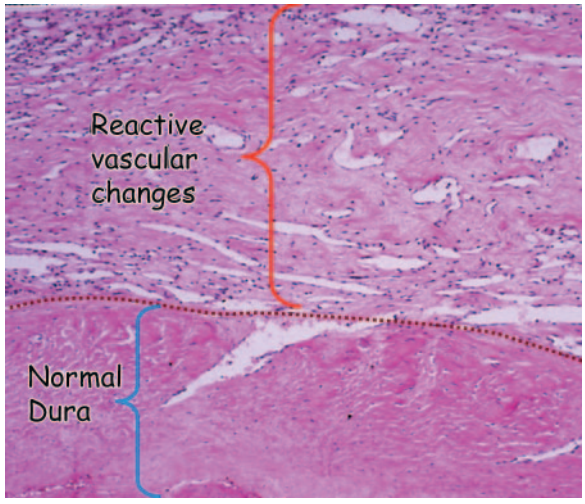

Figure 5. Dural tail tissue adjacent to meningioma. Lower portion of the photomicrograph (original magnification, ×250 ; hematoxylin-eosin [H-E] stain) shows normal dura mater that is largely collagen. The upper region shows reactive changes characterized by vascular congestion and loosening of the connective tissue. Slow flow within these vessels and accumulation of edema in the dura mater allow enhancement to be visualized on gadolinium-enhanced T1-weighted MR images.

detection and characterization of meningioma was very good (12). Contrast-enhanced MR imaging demonstrates a new finding (one not observed at CT): the *dural tail* or "dural flair." The dural tail is a curvilinear region of dural enhancement adjacent to the bulky hemispheric tumor (13–15) (Fig 4). The finding was originally thought to represent dural infiltration by tumor, and resection of all enhancing dura mater was thought to be appropriate (16). However, later studies helped confirm that most of the linear dural enhancement, especially when it was more than a centimeter away from the tumor bulk, was probably caused by a reactive process (17). This reactive process includes both vasocongestion and accumulation of interstitial edema, both of which increase the thickness of the dura mater (Fig 5).

Teaching Point

Because the dural capillaries are "nonneural," they do not form a blood-brain barrier, and, with accumulation of water within the dura mater, contrast material enhancement occurs.

Metastatic disease involving the dura mater most often arises from breast carcinoma in women and prostate cancer in men. Secondary CNS lymphoma is usually extraaxial and may be epidural, dural, subdural, subarachnoid, and combinations of these (Figs 6, 7).

Granulomatous disease, including sarcoid, tuberculosis, Wegener granulomatous, luetic gummas, rheumatoid nodules, and fungal disease, may each produce dural masses and may produce pachymeningeal enhancement. These granulomatous processes typically affect the basilar meninges, rather than involving the convexities of the cerebral hemispheres.

Leptomeningeal or Pia-Arachnoid Enhancement

Enhancement of the pia mater or enhancement that extends into the subarachnoid spaces of the sulci and cisterns is leptomeningeal enhancement

Figures 6, 7. **(6)** Mixed pachymeningeal and leptomeningeal enhancement in dural lymphoma. Axial gadolinium-enhanced MR images obtained with FLAIR **(a)** and T1-weighted **(b)** pulse sequences show superficial extraaxial enhancement adjacent to the right parietal and occipital lobes. The enhancement is both pia-arachnoid, which extends into the subarachnoid spaces of the sulci (arrowheads in **b**), and dura-arachnoid, which runs along the inner margin of the skull. **(7)** Dural (subdural) lymphoma. Operative photograph shows the dura mater (arrows). Under this tough connective tissue membrane is a soft cream-colored mass of lymphoma cells. The next membrane layer is the arachnoid, and much of the lymphoma is above it. Note, however, the few small areas with milky or cloudy discoloration, which can be seen through the arachnoid (arrowheads): These areas are subarachnoid lymphoma. Extraaxial lymphoma, such as this case, is almost invariably metastatic to the CNS, whereas primary lymphoma is typically intraaxial within the brain.

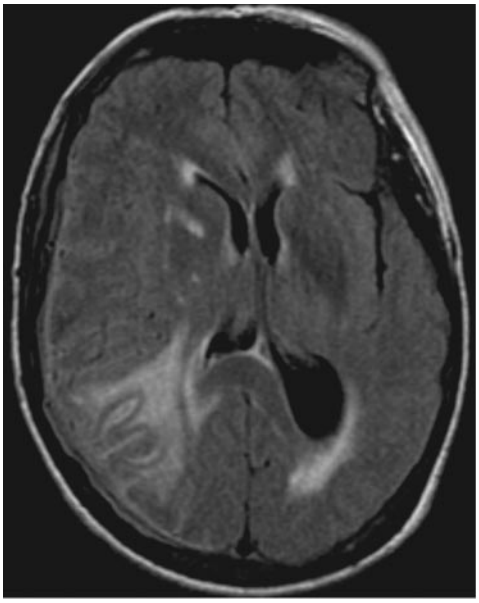

6a.

6b.

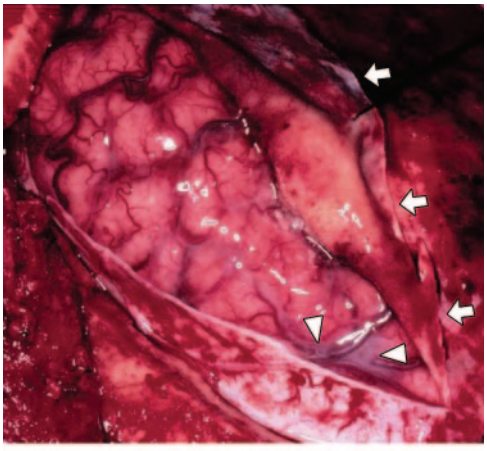

7.

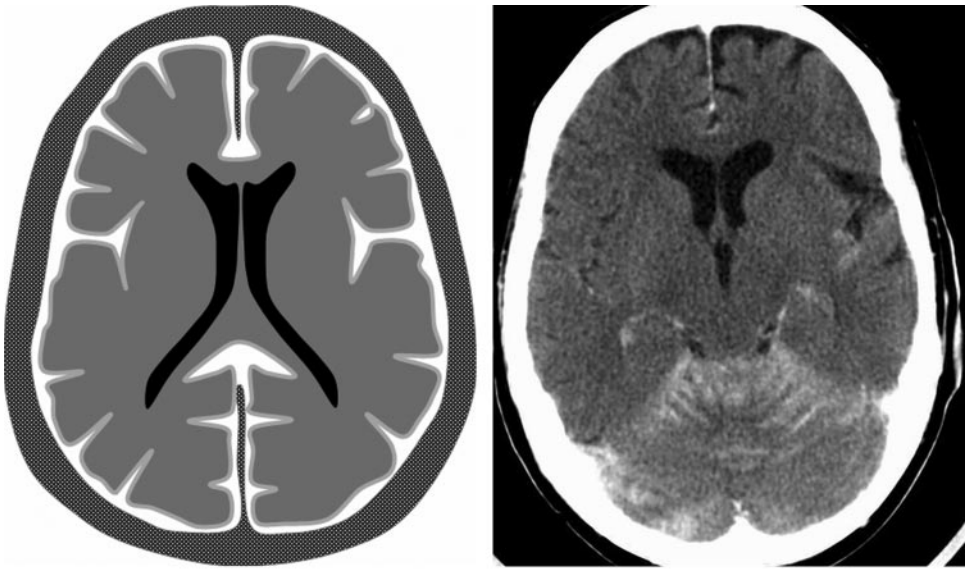

a. b.

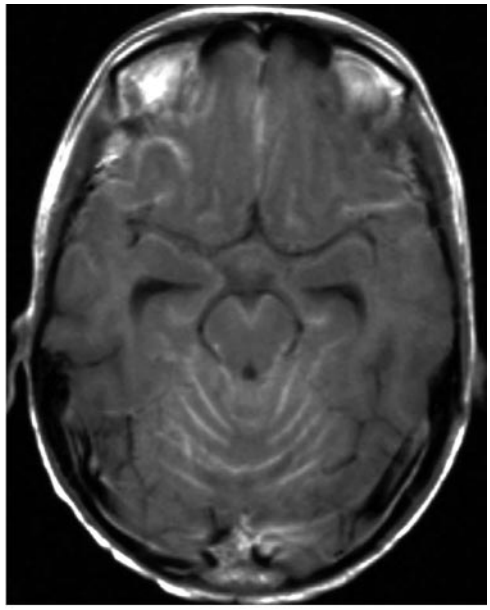

c.

Figure 8. Pia-arachnoid leptomeningeal enhancement. **(a)** Diagram illustrates the enhancement pattern, which follows the pial surface of the brain and fills the subarachnoid spaces of the sulci and cisterns. **(b, c)** Axial contrast-enhanced CT scan **(b)** and gadolinium-enhanced T1-weighted MR image **(c)** in a case of carcinomatous meningitis show pia-arachnoid enhancement along the surface of the brain and extending into the subarachnoid spaces between the cerebellar folia.

(Fig 8a). Leptomeningeal enhancement is usually associated with meningitis, which may be bacterial, viral, or fungal. The primary mechanism of this enhancement is breakdown of the blood-brain barrier without angiogenesis. Glycoproteins released by bacteria cause breakdown of the blood-brain barrier and allow contrast material to leak from vessels into the cerebrospinal fluid. Bacterial and viral meningitis exhibit enhancement that is typically thin and linear (Fig 9). The subarachnoid space is infiltrated with inflammatory cells, and the permeability in the meninges may increase because of bacterial glycoproteins released into the subarachnoid space (18) (Figs 9, 10). Fungal meningitis, however, may produce thicker, lumpy, or nodular enhancement in the subarachnoid space (1).

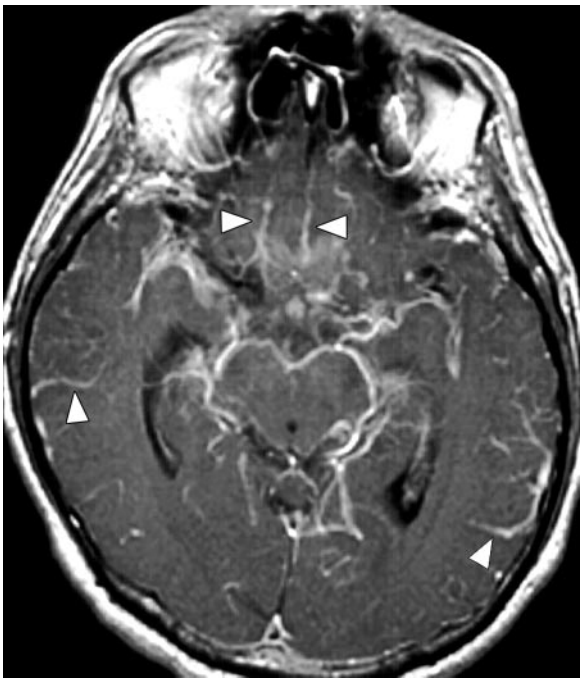

Figure 9. Pia-arachnoid leptomeningeal enhancement. Axial gadolinium-enhanced T1-weighted MR image shows relatively diffuse linear pial enhancement on the surface of the midbrain and subarachnoid space enhancement, which extends into multiple sulci (arrowheads).

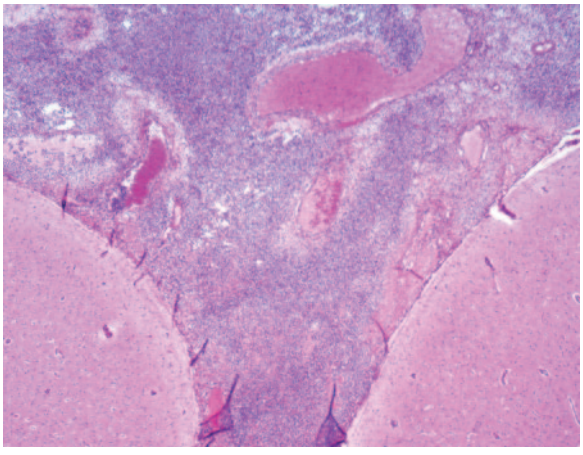

Figure 10. Pia-arachnoid leptomeningeal pattern in bacterial (*Streptococcus pneumoniae*) meningitis. Photomicrograph (original magnification, ×400; H-E stain) shows a dense inflammatory infiltrate along the surface of the brain that fills the subarachnoid space (center and top).

Neoplasms may spread into the subarachnoid space and produce enhancement of the brain surface and subarachnoid space, a pathologic process that is often called "carcinomatous meningitis" (Fig 8b, 8c). Both primary tumors (medulloblastoma, ependymoma, glioblastoma, and oligodendroglioma) and secondary tumors (eg, lymphoma and breast cancer) may spread through the subarachnoid space. Neoplastic disease in the subarachnoid space may produce thicker, lumpy, or nodular enhancement, similar to that of fungal disease (1). Despite the logic of these distinctions, carcinomatous meningitis can appear surprisingly thin and linear, as illustrated in our example (Fig 8b, 8c).

The patient's clinical presentation provides clues for the differential diagnosis, when fever or other signs of infection exist. Lumbar puncture may reveal a pleocytosis, and cerebrospinal fluid cultures may demonstrate the organism. Some cases of viral meningitis will be reported as "culture negative" or "sterile." Viral encephalitis (as well as sarcoidosis) may also produce enhancement along the cranial nerves, in addition to the brain surface. Normal cranial nerves never enhance within the subarachnoid space, and such enhancement is always abnormal. Primary nerve sheath tumors such as schwannoma may enhance in the subarachnoid space but are usually recognized as a lump or mass along the nerve.

Intraaxial Enhancement

Gyral Enhancement

Teaching Point

Superficial enhancement of the brain parenchyma is usually caused by vascular or inflammatory processes and is only rarely neoplastic (Fig 11). Vascular causes of serpentine (gyral) enhancement include vasodilatation after reperfusion of ischemic brain, the vasodilatation phase of migraine headache, posterior reversible encephalopathy

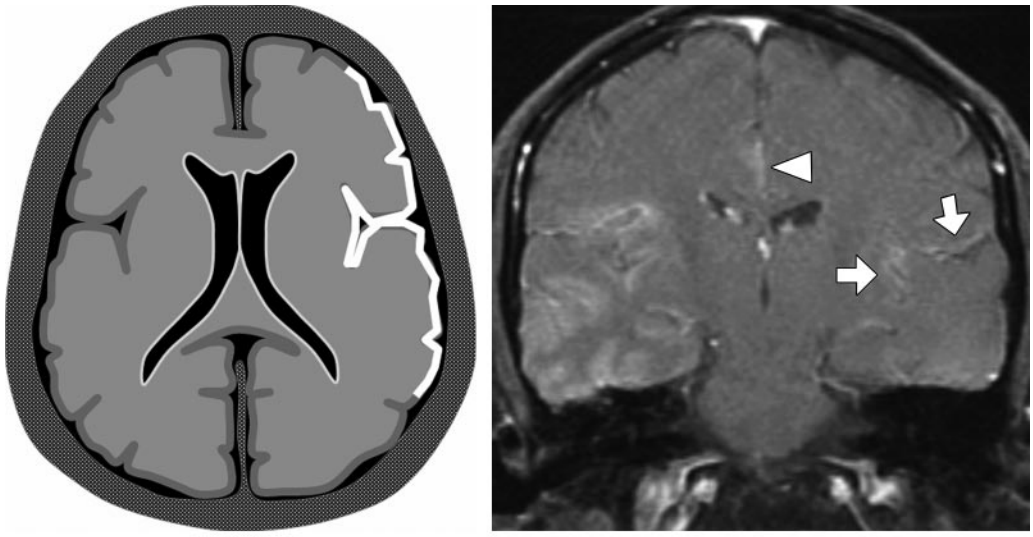

a. b.

Figure 11. Cortical gyral enhancement. **(a)** Diagram illustrates gyral enhancement that is localized to the superficial gray matter of the cerebral cortex. There is no enhancement of the arachnoid, and none in the subarachnoid space or sulci. **(b)** Coronal gadolinium-enhanced T1-weighted MR image in a case of herpes encephalitis shows multifocal, intraaxial, curvilinear, cortical gyriform enhancement that involves both temporal lobes. The enhancement is most prominent on the right but is also seen in the left insular region (arrows) as well as in the medial frontal lobes and cingulate gyrus (arrowhead).

syndrome (PRES), and vasodilatation with seizures (19–21). Serpentine enhancement from breakdown of the blood-brain barrier is most often seen in acutely reperfused cerebral infarction, subacute cerebral infarction, PRES, meningitis, and encephalitis. The primary distinction between vascular and inflammatory causes of the serpentine pattern of enhancement relies on correlation with clinical history and the region of enhancement. An abrupt onset of symptoms suggests a vascular cause, whereas a more indolent history and nonspecific headache or lethargy suggests inflammation or infection. Gyral lesions affecting a single artery territory are often vascular, whereas inflammatory lesions may affect multiple territories. The most common vascular processes affect the middle cerebral artery territory (up to 60% of cases). However, PRES lesions usually localize in the posterior cerebral artery territory (21–27).

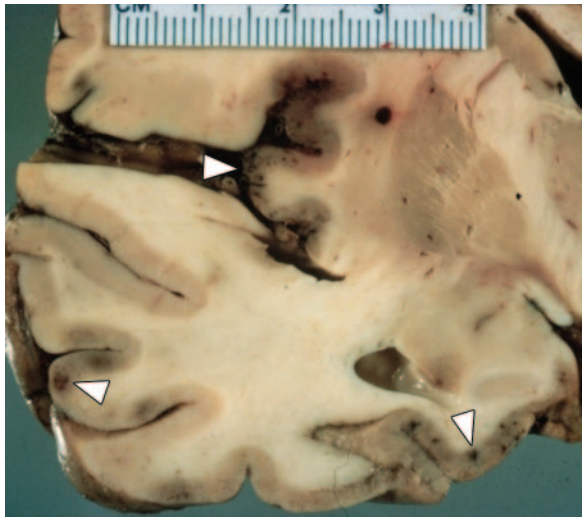

Figure 12. Herpes encephalitis. Photograph of a coronally sectioned gross specimen shows multiple petechial hemorrhages (arrowheads) and some granular atrophy of the insular cortex and the undersurface and medial temporal lobe. Scale is in centimeters.

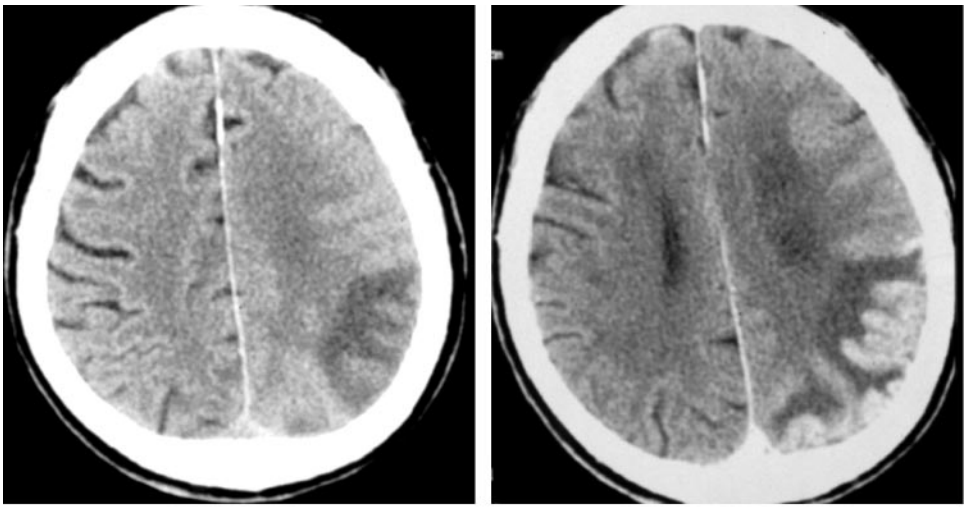

a. b.

Figure 13. Cortical gyral enhancement in embolic cerebral infarction in a 65-year-old woman. **(a)** On an axial nonenhanced CT scan, the sulci in the right hemisphere are normally prominent; on the left, the parietal sulci are effaced within a wedge-shaped region of abnormal hypoattenuation. The gyral surface is actually slightly hyperattenuating due to reperfusion injury with secondary petechial hemorrhage in the infarcted cortex. **(b)** Axial contrast-enhanced CT scan shows cortical gyral enhancement. The same endothelial damage that allows red cells to extravasate also permits contrast material to escape the vascular lumen and enter the brain parenchyma.

Herpes virus encephalitis produces superficial gray matter disease, changing signal intensity, and a breakdown of the blood-brain barrier to produce contrast enhancement in a cortical gyral pattern. Herpes encephalitis most often begins in the medial temporal lobes (uncus) and in the cingulate gyrus of the medial frontal and parietal lobes (Fig 11) (22–24,28). Pathologic specimens often show petechial hemorrhage and inflammation in these same locations (Fig 12). The lesion distribution is consistent with the hypothesis that herpes virus infection follows the olfactory pathways from the nasal cavity into the brain. The cortical-gyral enhancement in herpes encephalitis may lag behind the onset of signs and symptoms and may be suppressed by steroid medications; thus, the absence of enhancement does not exclude encephalitis.

Vascular gyral enhancement results from various mechanisms with variable time courses. The earliest enhancement can be caused by reversible blood-brain barrier changes when ischemia lasts for only several hours before reperfusion occurs (25,29–31). Early reperfusion may also produce vasodilatation, with increased blood volume and shortened mean transit time. These features were first observed at conventional angiography; they were described as dynamic changes and were called "luxury perfusion" because of the increased blood flow (32). The increased blood flow is caused by autoregulation mechanisms, which are "tricked" by the increased tissue P_{CO_2} that accumulates before reperfusion occurs. Ischemia or infarction may demonstrate gyral enhancement on both CT and MR images within minutes (with early reperfusion) (Fig 13). In the healing phases of cerebral infarction, from several days (5–7 days) to several weeks after the event, there will

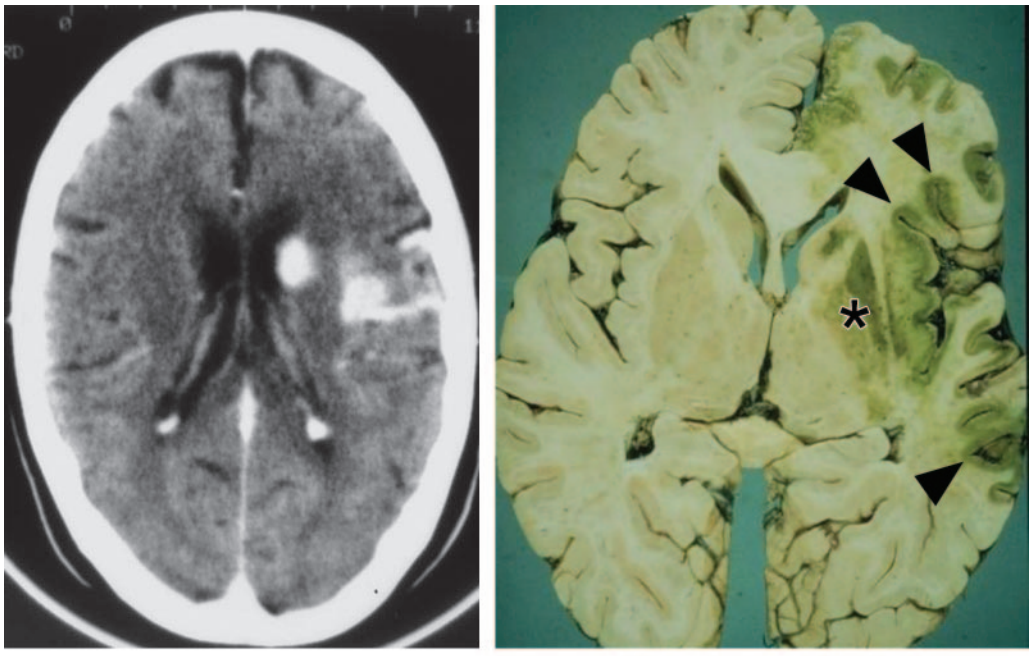

a. b.

Figure 14. Cortical gyral enhancement in subacute thrombotic cerebral infarction. **(a)** Axial contrast-enhanced CT scan shows enhancement that is limited to the opercular surfaces, insula, and caudate nucleus head (all of which are gray matter). **(b)** Photograph of an axially sectioned gross specimen shows green staining, which is caused by bilirubin bound to serum albumin, and which outlines areas of the brain where the blood-brain-barrier is no longer intact. Note how the green stain is almost exclusively in the gray matter of the cortex (arrowheads), basal ganglia (*), caudate nucleus, and claustrum. In these areas, the healing process would have removed the infarcted tissue, resulting in encephalomalacia and atrophy, if the patient had not died (the jaundiced patient died 2 weeks after left internal carotid thrombosis caused infarction of the anterior and middle cerebral artery territories).

be vascular proliferation or hypertrophy (Fig 14). Contrast enhancement usually fades away between 4 weeks and 4 months after the stroke, and enhancement is usually replaced by brain volume loss (33). The vascular changes facilitate the breakdown and removal of the dead brain tissue and lead to the encephalomalacia and atrophy characteristic of old "healed" infarction. The imaging appearance of postictal states may mimic the findings of cerebral infarction in several features, including gyral swelling, increased signal intensity on T2-weighted images and decreased signal intensity on T1-weighted images, sulcal effacement, and gyral enhancement (21). Reperfusion, whether acute (eg, after thrombolysis) or subacute to chronic ("healing" infarction), is required to deliver contrast material to produce enhancement.

Nodular Cortical and Subcortical Enhancement

A pattern of nodular enhancing lesions in subcortical and cortical parenchyma is typical for hematogenous dissemination of metastatic neoplasms and clot emboli. These lesions usually appear as small (<2-cm) circumscribed lesions near the gray matter–white matter junction (Figs 15, 16). Metastatic disease usually travels into the brain through the arteries and less commonly via the venous system. CNS metastases are distributed by blood flow, and the majority are supratentorial in the cerebral hemispheres, most often in the territory of the middle cerebral artery (34). Metastatic disease that follows venous pathways into the CNS usually arises from a primary pelvic malignancy and travels through the prevertebral veins of the Batson venous plexus. This venous route into the retroclival venous plexus partially accounts for the preferential distribution of some pelvic metastases into the posterior fossa (cerebellum and brainstem).

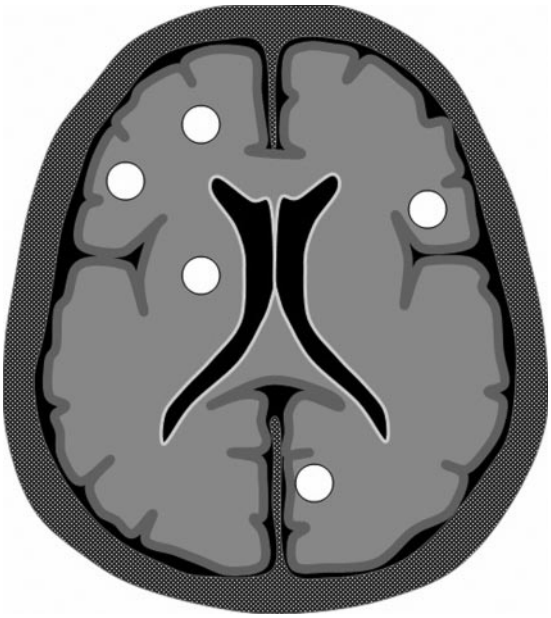

Figure 15. Subcortical nodular enhancement. Diagram illustrates nodular lesions near the gray matter–white matter junction and one near the deep gray matter. This pattern is typical for metastatic cancer and clot emboli. Because of their typical subcortical location, metastases often manifest with cortical symptoms or seizures while the lesions are small (often <1 cm in diameter).

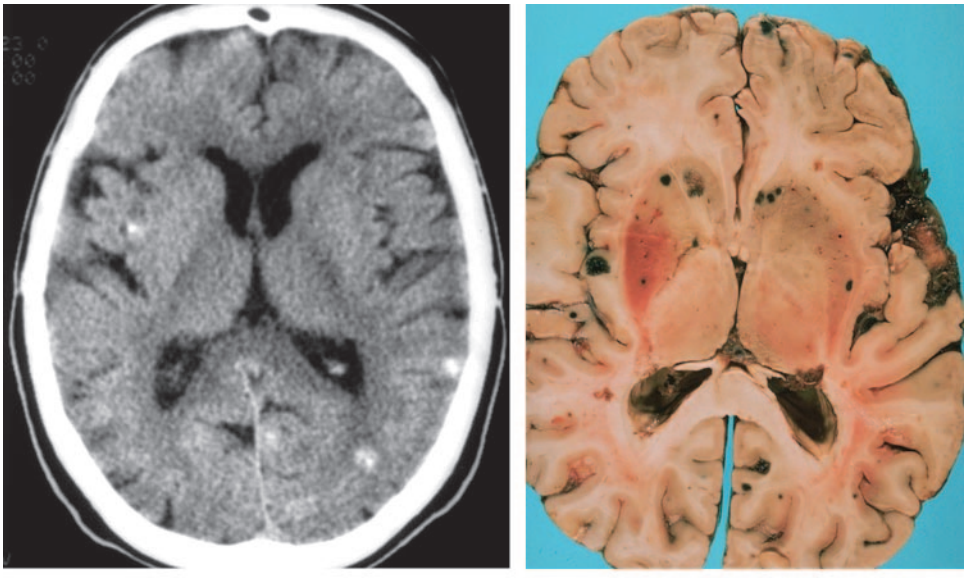

a. **b.**

Figure 16. Subcortical nodular enhancement in metastatic melanoma. **(a)** Axial nonenhanced CT scan demonstrates multiple nodular lesions that are hyperattenuating because of microscopic hemorrhages. **(b)** Photograph of an axially sectioned gross specimen shows black discoloration of these secondary (metastatic) melanoma nodules. The melanin pigment in these lesions makes them easy to see. The hematogenously disseminated lesions are all in or near the cortex, the gray matter–white matter junction, or deep gray matter of the basal ganglia; the greatest filtration of intravascular particulate material occurs in these areas.

Metastatic lesions are typically subcortical, occurring in or near the gray matter–white matter (corticomedullary) junction, whereas primary tumors are usually deeper (35). The subcortical gray matter–white matter pattern of nodule distribution reflects the filtration of intravascular particulate material in the region, where vessels branch and taper at the transition from the abundant vessels in the cortical gray matter into the relatively sparse vasculature of the white matter.

Tumor emboli must do more than disseminate through the vessel: The tumor must take hold and grow. Metastases usually are well demarcated, with a distinct "pushing margin" in gross pathologic specimens and on images (Fig 16). Angiogenesis allows the metastases to grow larger than 5 mm but also produces blood-brain barrier abnormality, which results in contrast enhancement and considerable perilesional vasogenic edema. Because of their typical location, cortical and subcortical metastases, even as small lesions, are likely to cause noticeable neurologic symptoms, including seizures. This characteristic is one of the reasons why metastases are typically first identified while they are solid nodular lesions, often 0.5–2.5 cm in diameter (Figs 15, 16). In contrast, primary glial tumors, such as low-grade and high-grade astrocytomas, arise away from the cortex and deep in the white matter, and they are usually much larger (2.5–5.0 cm in diameter) when they produce symptoms.

In approximately 40%–60% of cases of metastatic disease, routine contrast-enhanced CT and MR images will demonstrate a solitary metastatic lesion, although increasing the dose of contrast agent and using delayed imaging protocols may reveal additional metastatic lesions.

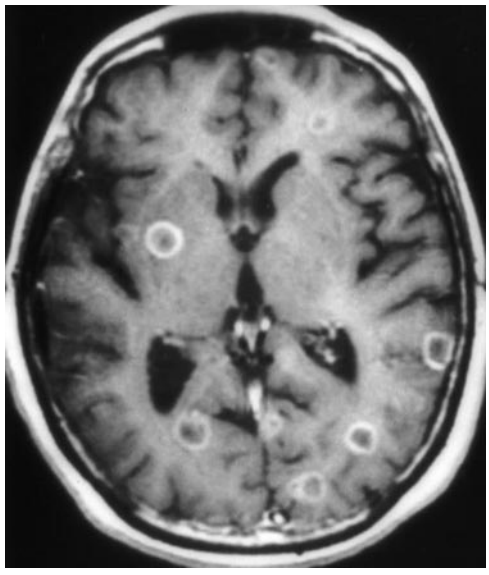

Figure 17. Subcortical nodular enhancement in metastatic breast cancer. Axial gadolinium-enhanced T1-weighted MR image shows multiple ring-enhancing lesions from necrosis of the metastases. The majority of these lesions are near the cortex or deep gray matter, with most being at the gray matter–white matter junction. This appearance is similar to those of septic emboli and abscesses, which indicates the need for good clinical correlation.

Deep and Periventricular Enhancement

Lesions near the gray matter–white matter junction are typical of hematogenous spread, as discussed in the previous section. Lesions that manifest deeper within the cerebral hemispheres usually have other causes. These deeper subcortical lesions may involve the white matter, the deep gray nuclei (eg, basal ganglia, thalamus), or both white and gray matter. Metabolic diseases and toxins may preferentially damage the deep gray matter. Various diseases that affect myelin production or repair primarily damage the white matter. Most leukoencephalopathies become destructive during their natural evolution and lead to a decreased volume of affected white matter.

These changes may produce alterations of increased water signal intensity on MR images and decreased attenuation on CT images. Many pathologic processes will produce enhancement with localization similar to the signal change pattern. We look for these clear-cut distinctions between deep white matter lesions and deep gray matter lesions as a guide to differential diagnosis. However, many diseases affect both the gray matter and the white matter in the deep periventricular region, and some of these are more common in immunocompromised patients, such as those with toxoplasmosis and primary CNS lymphoma.

Deep Ring-enhancing Lesions

Ring-enhancing lesions may be superficial, but they are usually subcortical or deep. Schwartz et al (36) reviewed 221 ring-enhancing lesions seen

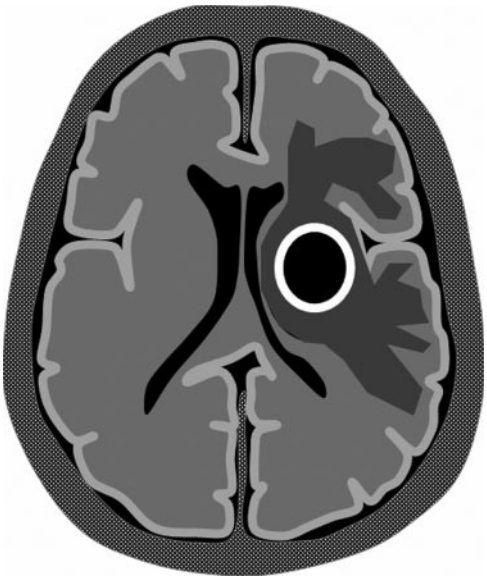

Figure 18. Smooth ring-enhancing pattern in late cerebritis and subsequent cerebral abscess. Diagram illustrates a thin (<10 mm) rim of enhancement, which is usually very smooth along the inner margin; this pattern is characteristic of an abscess. The lesion is surrounded by a crown of vasogenic edema spreading into the white matter.

on MR images and reported that 40% were gliomas; 30%, metastases; 8%, abscesses; and 6%, demyelinating disease. In their series, 45% of metastases and 77% of gliomas were single lesions, whereas abscesses and multiple sclerosis lesions were multiple in 75% and 85% of patients, respectively (36). Both necrotic metastases and hematogenous abscesses typically manifest as cortical or subcortical lesions with cavitation. Metastatic deposits are often solid nodular lesions that may become ring-enhancing because of necrosis (eg, after chemotherapy or irradiation) (Fig 17). Multiple cortical or subcortical ring-enhancing lesions have an infectious etiology (ie, they represent brain abscesses) in patients with subacute bacterial endocarditis, indwelling catheters, or other implanted devices such as cardiac valves. Deep white matter ring-enhancing lesions, especially those with mass effect and surrounding vasogenic edema, are most often either primary neoplasms (eg, glioblastoma multiforme) or abscesses (Fig 18).

Cerebritis and Abscess

Pyogenic infections of the CNS usually arise from septic emboli transmitted hematogenously. Less frequently, transdural spread may occur from adjacent sinus infections (sphenoid, ethmoid, frontal, and mastoid air cells). After an initial unorganized inflammation or cerebritis, the successful immune response will include angiogenic neovascularity and collagen deposition (ie, a capsule of granulation tissue) and formation of an abscess. A layer of astrogliosis surrounds the granulation tissue (37,38). Ring enhancement in an abscess reflects the granulation tissue in its wall that has both increased vascularity and abnormally permeable capillaries. Collagen in the wall reinforces it to localize and confine the infected brain and pus. Preceding this organized abscess stage is cerebritis. Cerebritis is an acute inflammatory reaction with altered permeability of the native vessels but without angiogenesis or neovascularity. Before angiogenesis, the signal intensity and attenuation changes are directly caused by the inflammatory process, and perilesional vasogenic edema is variable and may be minimal. In the immunocompetent patient, cerebritis progresses to form an organized abscess. An intermediate stage of transition from cerebritis to an organized abscess may be suspected when the lesion does not have a sharp margin or a wall that is less discrete (Fig 19). On initial CT and MR images, cerebritis will appear as a ring-enhancing lesion (Fig 19a–19c). In cerebritis without a collagen capsule, images obtained over 20–40 minutes may show "fill-in" of the ring center (39). This "filling-in" does not occur in a well-organized abscess and suggests cerebritis (39). Cerebritis is often treated nonsurgically with high-dose antibiotics.

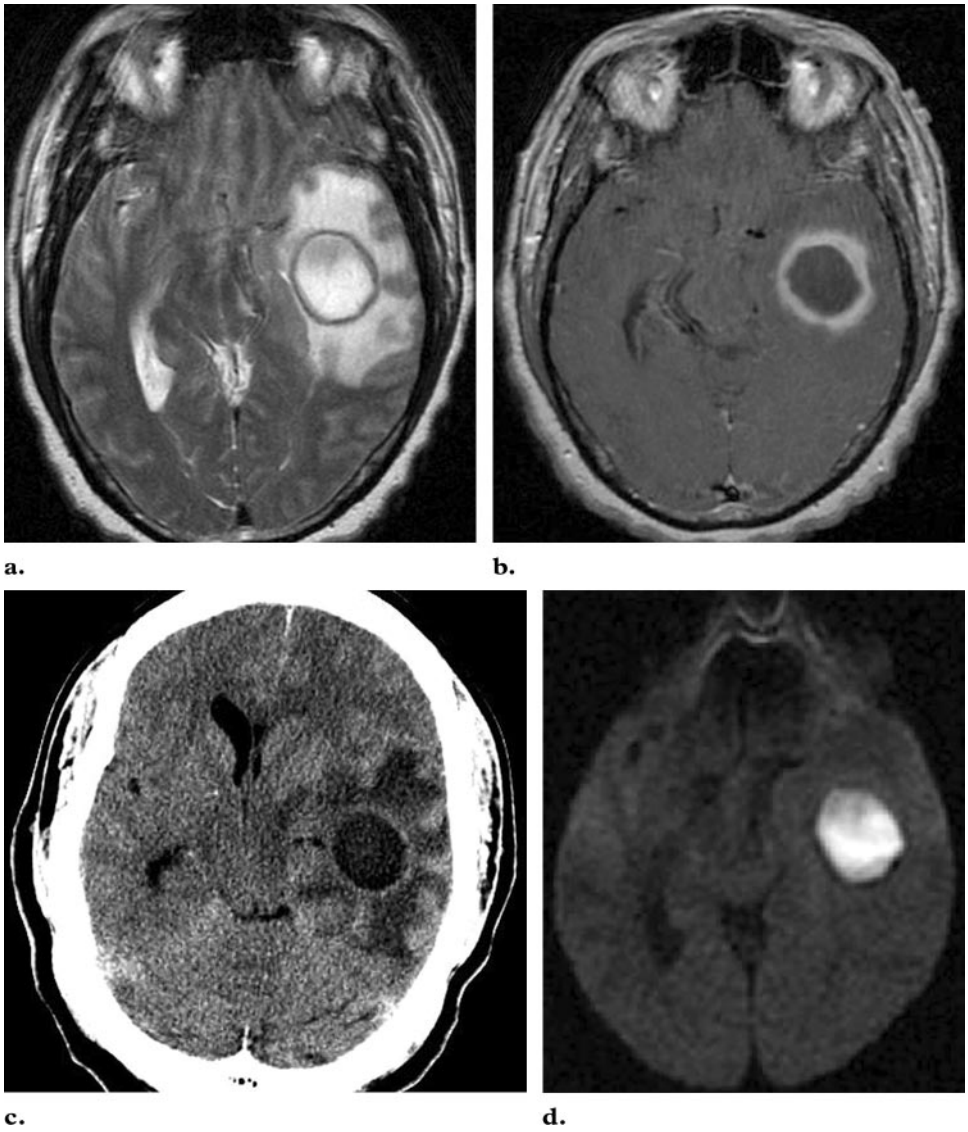

Figure 19. Smooth ring-enhancing pattern in late cerebritis and subsequent cerebral abscess. **(a)** Axial T2-weighted MR image shows a circular mass with extensive perilesional vasogenic edema that surrounds a dark rim (the abscess wall). Mild mass effect on the midline structures is seen. **(b)** On an axial gadolinium-enhanced T1-weighted MR image, the inner wall of the ring-enhancing lesion is smoother than the slightly irregular outer wall. This appearance reflects an earlier stage in the organization of the infection, as it makes the transition from cerebritis to abscess, since a more organized abscess will appear smoother. **(c)** Axial CT scan shows a sharply marginated, ringed lesion with surrounding perilesional vasogenic edema. **(d)** On an axial diffusion-weighted MR image, the lesion has markedly restricted diffusion (hyperintensity) due to the viscous pus and necrotic brain tissue in the abscess core.

An abscess is the result of organization and partial neutralization of an infection. In the brain, an abscess may develop a well-formed capsule in 2–4 weeks. The organizing infection forms concentric zones or layers (37–39) (Fig 20): *(a)* necrotic brain in the innermost layer, *(b)* reactive white cells (macrophages, monocytes) and fibroblasts, *(c)* capillary vascular proliferation and collagen capsule formation, *(d)* neovascularity and active cerebritis, and *(e)* reactive astrogliosis and vasogenic edema in the outer margin.

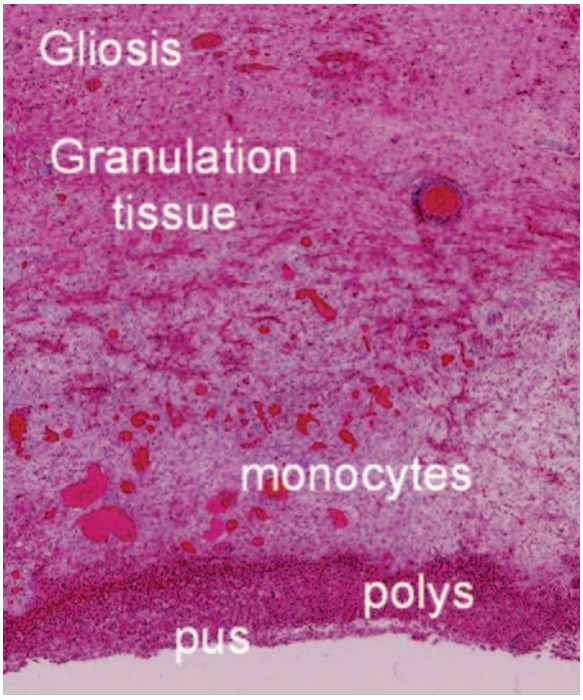

Figure 20. Brain abscess. Photomicrograph (original magnification, ×250; H-E stain) shows the microscopic layers from top to bottom: reactive gliosis and the brain margin, vascular proliferation with collagen formation (granulation tissue), migrating white blood cells (monocytes), and pus. *polys* = polymorphonuclear leukocytes (Courtesy of Joseph Parisi, MD, Mayo Clinic, Rochester, Minn.)

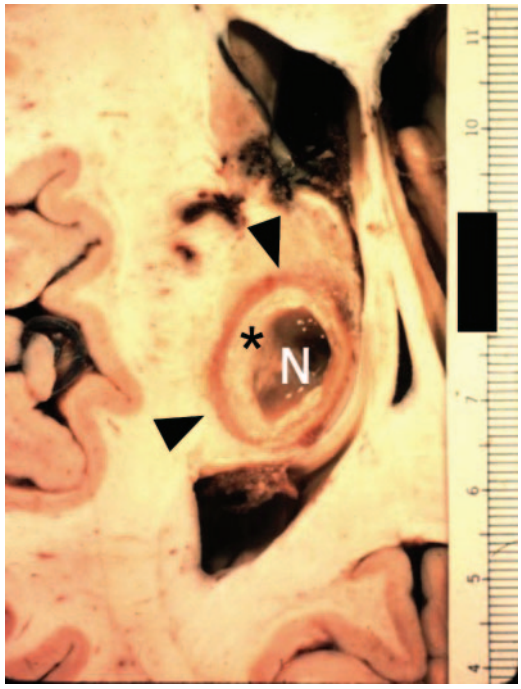

Figure 21. Cerebral abscess in a patient with AIDS who died of multiple brain abscesses from *Toxoplasma gondii*. Photograph of an axially sectioned gross specimen shows an abscess in the thalamus with three macroscopic zones: a reddish region of neovascularity (arrowheads), a white region of extravascular white cells and pus (*), and an inner zone of liquefaction necrosis *(N)*. Liquefaction necrosis occurs in lipid-rich organs (such as the brain), when an exuberant leukocytic reaction brings lytic enzymes into the infected region. Scale is in centimeters.

Teaching Point

The rim of reactive tissue is usually thin (2–7 mm), uniformly convex, and smooth on both the outer and inner aspects (Fig 21).

The ring-enhancing lesion of a cerebral abscess is classically described as having a smooth inner margin and a smooth outer margin. However, in some examples, especially during the transition from cerebritis to abscess, the outer rim of enhancement may resemble the corona of a solar eclipse (Fig 18b). An abscess rim is typically hypointense on T2-weighted MR images, and a variety of explanations have been proposed, including dense collagen, blood products (hemosiderin), and paramagnetic free radicals (eg, atomic oxygen produced by leukocytes that are attacking the bacteria) (40). Almost 90% of abscesses demonstrate a hypointense rim, and 75% form a continuous hypointense rim (36). The abscess wall often appears thicker on the gray matter or "oxygen side" of the ring and thinner along the white matter or ventricular side. The thinner margin of the deep or medial aspect of the lesion is predisposed to daughter abscess formation and deep rupture of the abscess into the ventricle (which leads to pyocephalus and high mortality).

Occasionally, the outer perimeter of the abscess wall can appear irregular. The enhancement is both interstitial (from increased capillary permeability) and intravascular (from increased perfusion in the granulation tissue). The interstitial contrast material usually does not migrate into the center of an abscess cavity, even on delayed images, because of the viscosity of the pus and liquefaction necrosis. The viscosity of the necrotic center also explains its high signal intensity on diffusion-weighted images (Fig 19d) and corresponding reduced diffusion coefficient and therefore low signal intensity on the apparent diffusion coefficient maps.

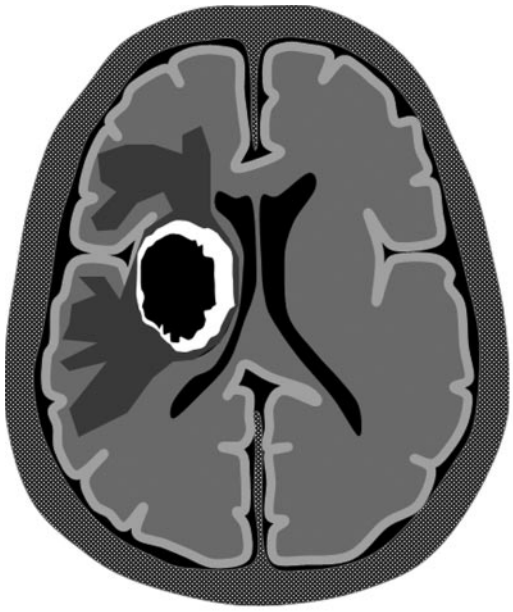

a.

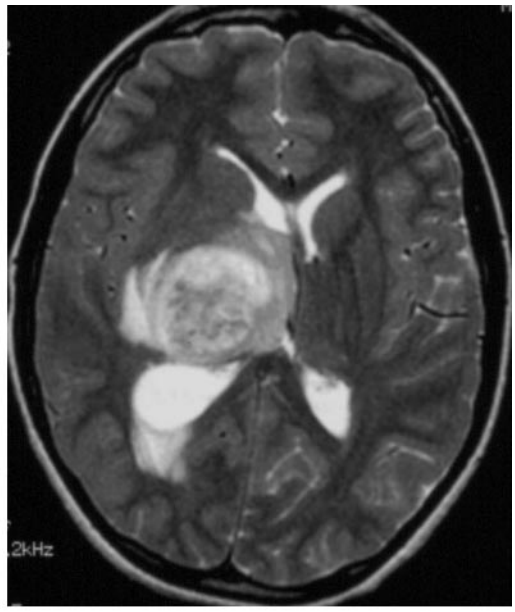

b.

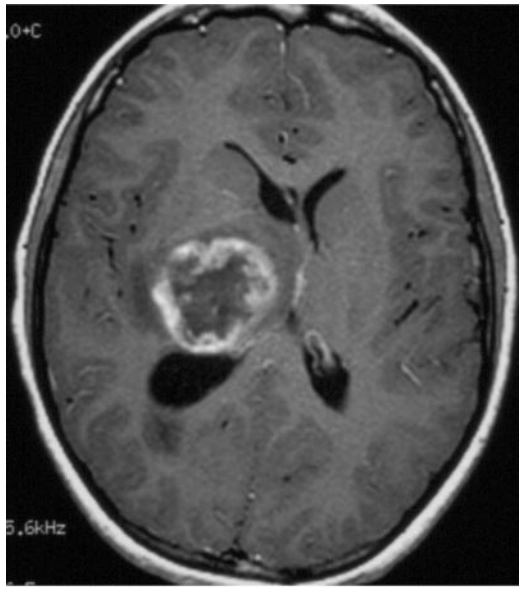

c.

Figure 22. Necrotic ring pattern of high-grade neoplasms. **(a)** Diagram illustrates a lesion with an enhanced rim that is very thick medially; the ring is thicker and more irregular than that seen in a typical abscess. The lesion is surrounded by a crown of vasogenic edema spreading into the white matter. **(b, c)** Glioblastoma multiforme. **(b)** Axial nonenhanced T2-weighted MR image shows a large heterogeneous mass that displaces the frontal horn of the lateral ventricle. **(c)** Axial gadolinium-enhanced T1-weighted MR image shows the irregular, heterogeneous ring-enhancing mass. The ring has a characteristically undulating or wavy margin, and its inner aspect is shaggy and irregular.

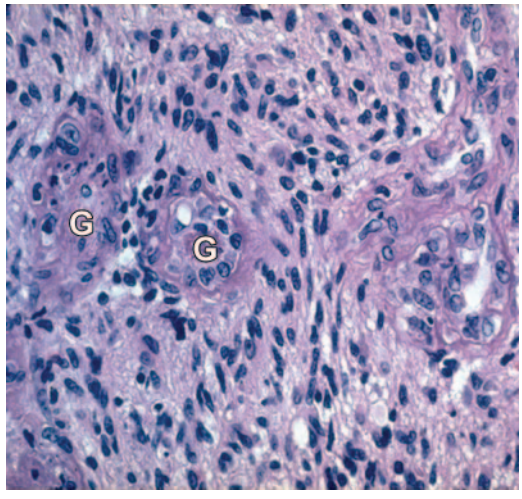

Figure 23. Glioblastoma multiforme. Photomicrograph (original magnification, ×250; H-E stain) shows vascular proliferation with thick-walled capillaries, which are called *glomeruloid vessels (G)* because they resemble the tuft of vessels in the renal glomeruli.

Figure 24. Glioblastoma multiforme. **(a)** Axial contrast-enhanced CT scan shows a mass with a complex appearance. The outer cortical region of the tumor (*) has a thick irregular rim with a shaggy inner margin (an appearance that is more typical of a glioblastoma multiforme). The relatively smooth and thin deep inner margin mimics the thin reactive rim of an abscess wall. **(b)** Lateral angiogram, obtained after an internal carotid injection, shows a large, hypervascular mass with irregular vascularity, pooling of contrast material, and early draining veins (arrows). Early draining veins are the angiographic sign of a short mean transit time (MTT). Modern MR perfusion imaging would also demonstrate increased perfusion (elevated rCBV and rCBF) and a shortened MTT. **(c)** Photograph of a coronally sectioned gross specimen shows the outer cortical region of the tumor with the more typical, thick irregular rim (*) and shaggy inner margin and the relatively smooth, thin, deep inner margin (arrows). Within the neoplasm is a region of hemorrhagic necrosis. Scale is in centimeters.

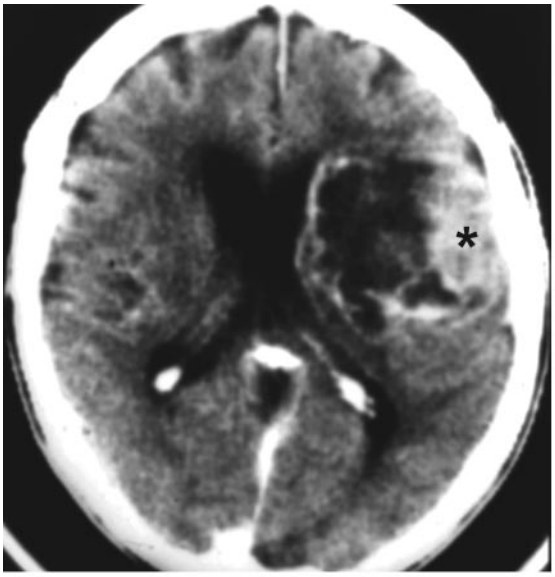

a.

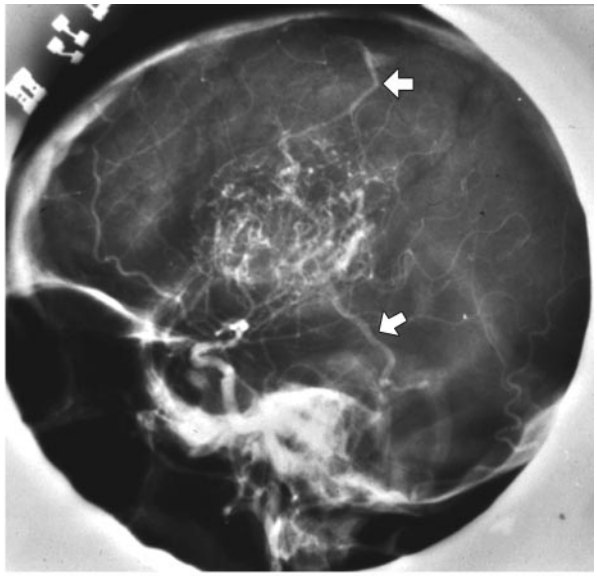

b.

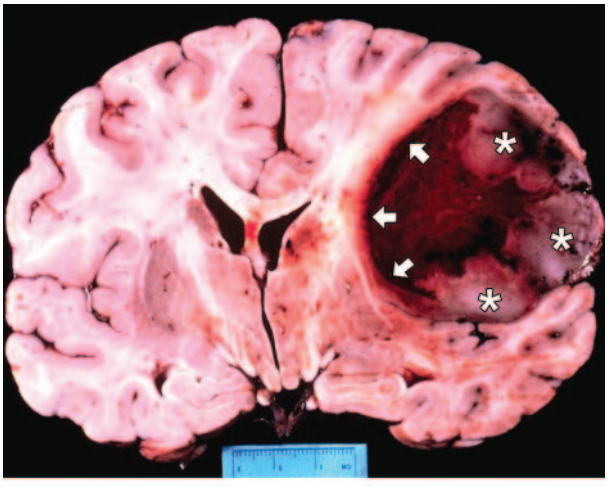

c.

Necrotic High-grade Primary Neoplasms

Necrotic neoplasms are usually, but not exclusively, malignant, and they may be primary or metastatic. Imaging features of a necrotic neoplasm include a thick irregular ring with a shaggy inner margin, multilocular and complex ring patterns, and a wall that is thicker than 10 mm (at least in some areas) (Fig 22). Deep lesions with this pattern—especially when they are located in the corpus callosum and thalamus—are usually primary astrocytic glial neoplasms. In adults, such lesions are usually diffusely infiltrating astrocytomas, with 60% being higher grade (ie, WHO grade 4 astrocytoma or glioblastoma multiforme).

Teaching Point

High-grade primary tumors, exemplified by glioblastoma multiforme, are usually microscopically necrotic and macroscopically cavitating (41–43). They may form unilocular lesions, but more often they are complex, multilocular, thick-walled, ring-enhancing masses. A glioblastoma multiforme characteristically has prominent neovascularity with abnormal blood-brain barrier (Fig 23). The enhancing rim, which contains the greatest concentration of neovascularity, is often thick, is wavy or undulating, and has a shaggy inner margin. Because the tumor vessels sprout from preexisting normal vasculature, the enhancing rim may be thicker on the cortical or outer surface, compared with the thinner, deep or white-matter margin (Fig 24). On delayed images,

some glioblastomas multiforme show progressive enhancement inside the rim, usually in a patchy pattern. This pattern reflects the presence of islands of surviving tumor cells within regions undergoing macroscopic necrosis. High-grade tumors are characterized on MR images by increased perfusion and a shortened mean transit time. Angiogenesis in most high-grade gliomas is stimulated by vascular endothelial growth factor (44,45). Neovascularity is mandated by the high metabolic rate and close cellular packing of the tumor cells. The abnormal tumor vessels include arteries, veins, and capillary endothelium that have intercellular gaps and a discontinuous basement membrane (Fig 23). Both intravascular, flow-related enhancement and interstitial, permeability-related enhancement are prominent.

Fluid-secreting Low-grade Primary Neoplasms

Fluid-secreting primary neoplasms are typically well-marginated and usually of low histologic grade. The margins of these "cystic" fluid-secreting masses show either a nodular or partial rim of enhancement. Examples include the familiar pilocytic astrocytoma and hemangioblastoma, both of which are seen most often in the cerebellum (Fig 25). Among lesions occurring above the tentorium cerebelli, pilocytic astrocytoma, pleomorphic xanthoastrocytoma, ganglioglioma, and extraventricular ependymoma may also manifest as mixed solid and fluid lesions. The term *cystic* should be avoided because a true cyst is a fluid-filled space lined by an epithelium. In most fluid-secreting neoplasms, part of the rim around the fluid does not enhance because it is compressed or gliotic tissue, rather than neoplastic tissue. In fact, the appearance of a fluid space with an incomplete ring is very suggestive of a fluid-secreting—and therefore usually benign—primary neoplasm.

High-grade neoplasms become heterogeneous because of geographic areas of necrosis that may coalesce into "central necrosis." In contrast, some low-grade neoplasms become heterogeneous because of leakage or secretion of fluid, as distinct from necrosis. The fluid may have high or low viscosity and variable penetration of contrast material into the fluid core. Most low-grade primary neoplasms do not produce an increase in arterial

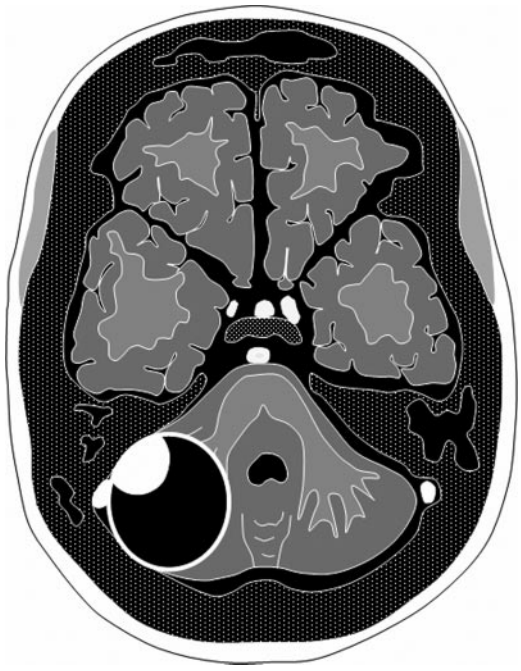

Figure 25. Fluid-secreting neoplasm (cyst with mural nodule pattern). Diagram illustrates a "cystic" mass with a "mural nodule," which is the classic description for a pilocytic astrocytoma. This pattern is seen in a variety of fluid-secreting neoplasms, including hemangioblastoma, ganglioglioma, and pleomorphic xanthoastrocytoma.

vessels and do not show increased perfusion, although they may have increased metabolism (46). However, they have abnormal capillaries with increased permeability and an absent blood-brain barrier, characteristics that result in leakage of fluid and contrast material (47). The fluid may form microcysts (Fig 26) within the "solid" tumor nodule, before forming a larger fluid collection that creates the "cyst-with-nodule" appearance (Fig 27). Most fluid-secreting tumors show enhancement limited to the mural nodule, whereas some may demonstrate a nodule with partial rim enhancement (a variant of the open ring sign). Although the gliotic margin often does not enhance, it may show enhancement on delayed images or with higher doses of contrast material. Because fluid may be present within, as well as outside or adjacent to the nodule, many of the so-called cyst-with-nodule lesions actually have a more complex shape. For example, only about one-third of hemangioblastomas actually have a unilocular fluid space with a single mural nodule (48). The majority of hemangioblastomas show a more complex pattern, ranging from mostly solid to mostly fluid. With their improved spatial reso-

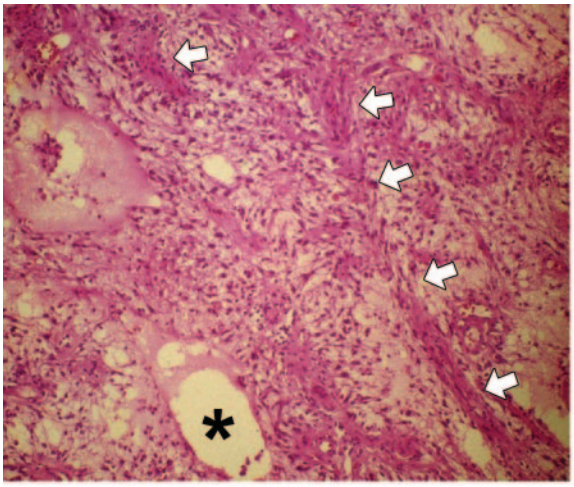

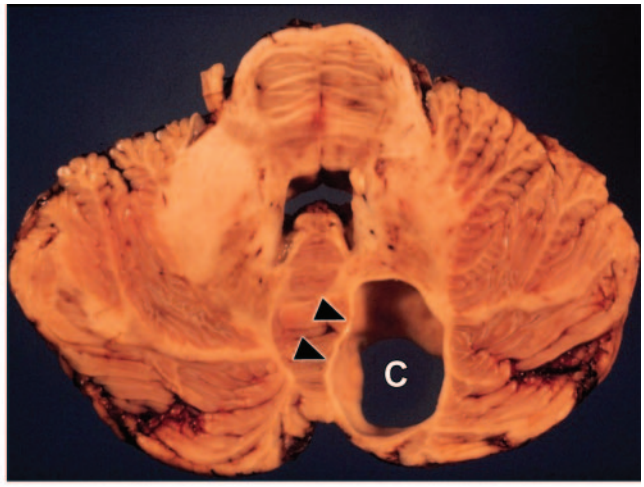

26. 27.

Figures 26, 27. Pilocytic astrocytoma. **(26)** Photomicrograph (original magnification, ×400; H-E stain) shows the typical biphasic pattern of alternating dense regions (arrows) and loose areas with microcysts (*). **(27)** Photograph of an axially sectioned gross specimen of the cerebellum clearly shows the tumor fluid cavity *(C)* with a surrounding thin (<2-mm) region of nonneoplastic reactive gliosis (arrowheads).

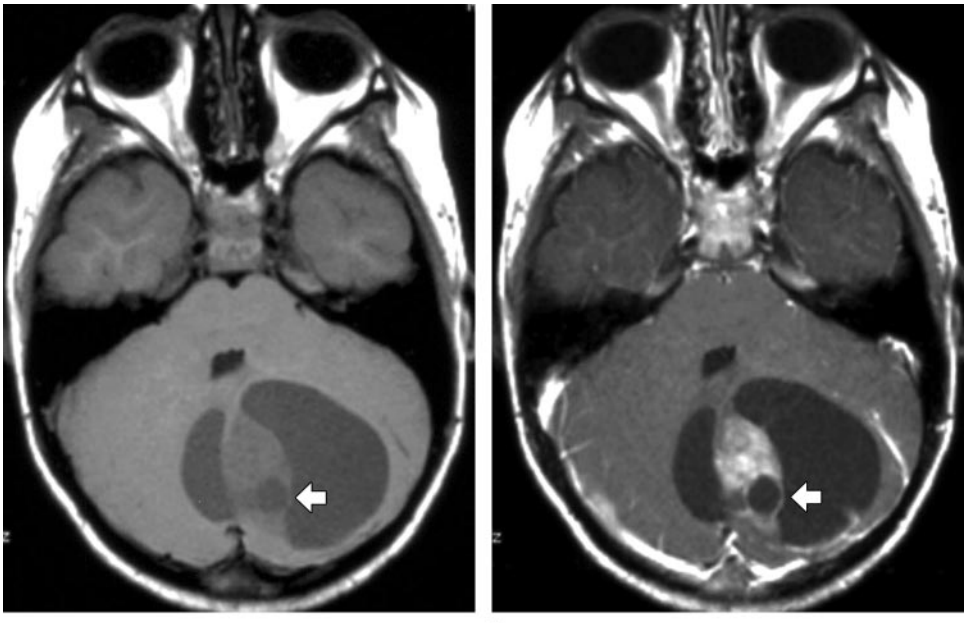

a. b.

Figure 28. Pilocytic astrocytoma. **(a)** Axial nonenhanced T1-weighted MR image shows a smooth-margined mass in the cerebellum surrounded by a cyst with fluid that is higher intensity than the cerebrospinal fluid in the fourth ventricle. **(b)** Axial gadolinium-enhanced T1-weighted MR image shows intense enhancement of the mural nodule, but the rim surrounding the fluid secreted by the tumor does not enhance. A cystic mass with a mural nodule in the cerebellum is classic for a pilocytic astrocytoma. Note that this example has three fluid collections and that one of them (arrow) is actually inside the tumor nodule.

lution, both MR imaging and CT have demonstrated that the most common cyst-with-nodule neoplasm, the pilocytic astrocytoma, often has more complex morphology, with fluid within the solid nodule and adjacent to it (Fig 28). Fluid-secreting neoplasms may, therefore, demonstrate an incomplete ring of enhancement, because part of the margin surrounding the fluid is neoplastic and part is nonneoplastic (compressed or gliotic brain tissue). Occasionally, thin (<2-mm) rim enhancement, representing gliosis and not neoplastic tissue, can be seen in a pilocytic astrocytoma (49).

Teaching Point

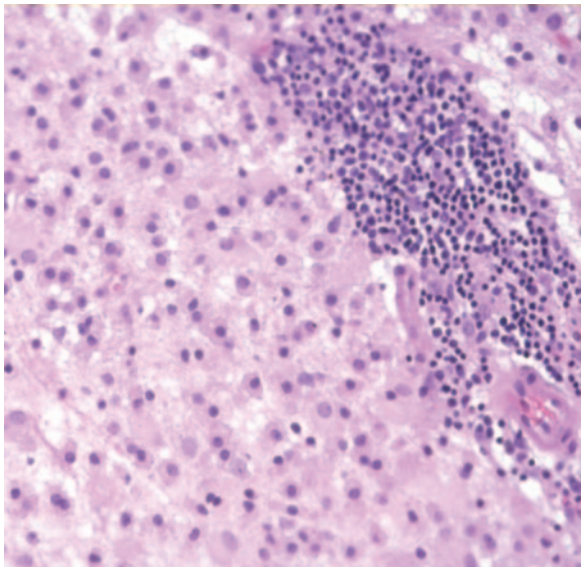

Figure 29. Demyelination (multiple sclerosis). Photomicrograph (original magnification, ×400; H-E stain) shows a perivascular infiltrate of inflammatory cells in the upper right corner but no angiogenesis.

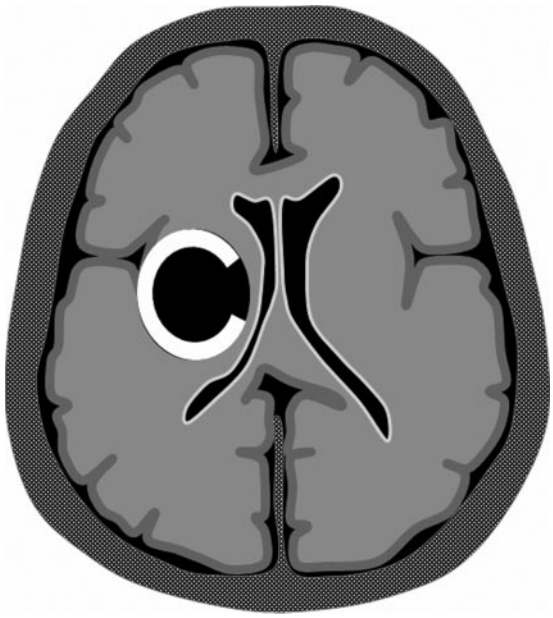

Figure 30. Open ring pattern. Diagram illustrates a lesion with an incomplete rim (only part of the rim enhances). This appearance may be seen in multiple sclerosis (without mass effect as in this drawing), tumefactive demyelination (with mass effect), and fluid-secreting neoplasms (with associated mass effect and occasionally with surrounding vasogenic edema).

Demyelination

The most common cause of demyelination is multiple sclerosis. The diagnosis of multiple sclerosis includes some demonstration, by clinical or radiologic means, that lesions are separated in both space and time. Classic multiple sclerosis lesions or plaques are easy to recognize as elongated oval regions of increased water that are oriented perpendicular to the margins of the lateral ventricles. Multiple sclerosis plaques enhance during the "active phase," and this enhancement usually lasts for 2–6 weeks and only rarely longer (50). The cause of the enhancement in demyelination is inflammation, usually perivascular, which most often is limited to the venous side (ie, "perivenular" inflammation); there is no neovascularity, no angiogenesis, and no necrosis (51) (Fig 29). For this reason, enhancement of multiple sclerosis plaques may be faint, the lesions usually do not produce any perilesional vasogenic edema, and the enhancing rim is thin and often incomplete (36,52,53) (Fig 30). This appearance may usually be distinguished from those of an abscess (which has surrounding vasogenic edema), a necrotic neoplasm (which has a thick rim), and a fluid-secreting tumor (which has free fluid, rather than altered white matter, inside the rim) (Fig 31). Masdeu et al (53) reported that although an open ring sign may be seen in abscess and neoplasm, it is strongly suggestive of demyelination. An "incomplete ring" may be seen in active demyelination, both in multiple sclerosis and in tumefactive demyelination (52,53). If multiple sclerosis is suspected, MR imaging of the spinal cord may demonstrate additional lesions to help support the diagnosis (54).

Deep Lesions: Periventricular Pattern

The common causes of a periventricular enhancement pattern include primary CNS lymphoma, primary glial tumors, and infectious ependymitis (Fig 32).

Primary CNS lymphomas are malignant B-cell tumors. Historically, lymphoma rarely involved the CNS; however, with the increasing prevalence of conditions that cause immunosuppression, such as acquired imummodeficiency syndrome (AIDS) and immunosuppressive therapies, the frequency of primary CNS lymphoma has risen dramatically. Primary CNS lymphoma usually

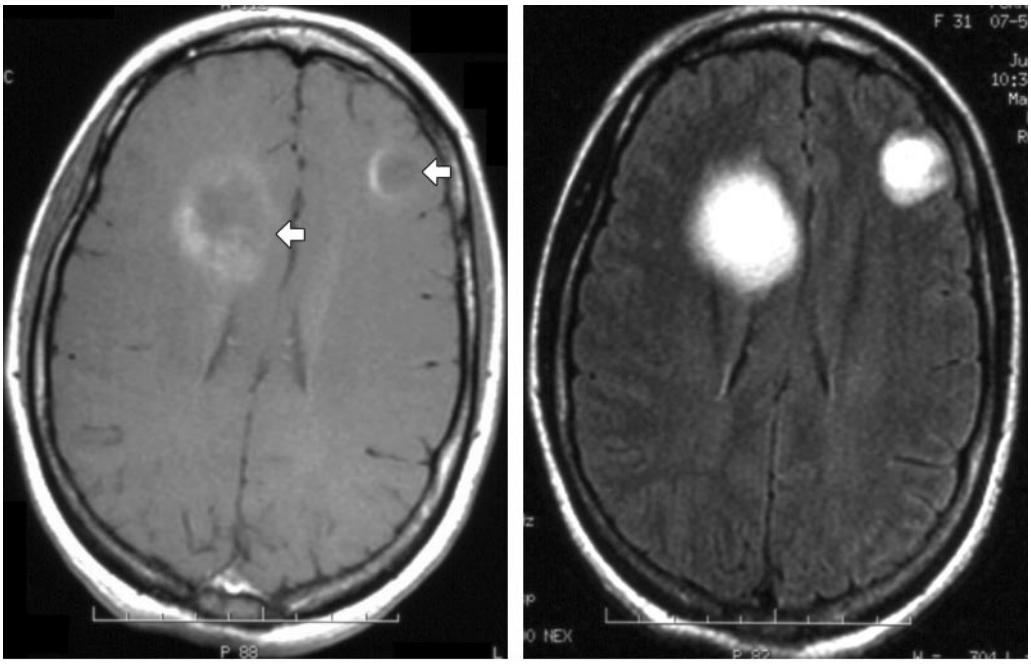

a. b.

Figure 31. Demyelination. **(a)** Axial gadolinium-enhanced T1-weighted MR image shows two rimmed lesions; neither has a completely circumferential rim of enhancement (arrows). The left frontal lesion has a more conspicuous open ring sign. Note the absence of surrounding vasogenic edema—another potential differential feature to distinguish demyelination from both abscess and neoplasm. **(b)** Axial T2-weighted MR image shows the two homogeneous, hyperintense lesions and the conspicuous absence of vasogenic edema.

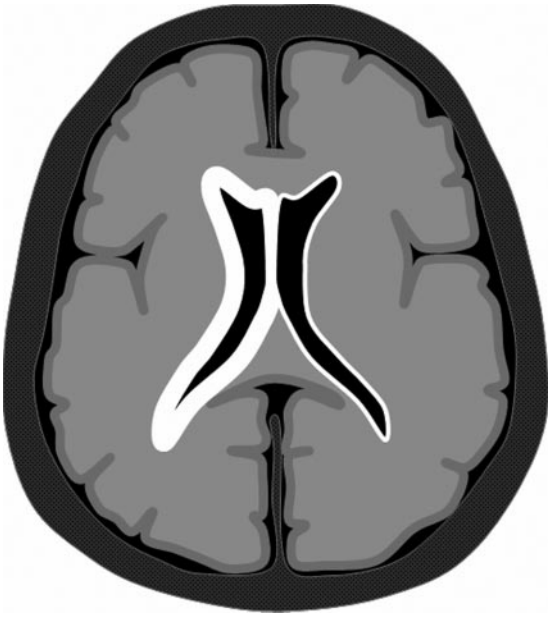

Figure 32. Periventricular pattern. Diagram illustrates thick periventricular enhancement, as shown around the right lateral ventricle. This enhancement pattern is usually neoplastic and is most commonly seen in a high-grade astrocytoma or primary CNS lymphoma. Thin periventricular enhancement, as shown around the left lateral ventricle, is usually infectious.

occurs as a solitary supratentorial mass, but a substantial minority of these cases manifests as multiple lesions or in the cerebellum and brainstem. Primary CNS lymphoma commonly manifests as bulky, sharply demarcated, deep cerebral hemisphere masses with mild to moderate surrounding cerebral edema. The periventricular pattern of enhancement is typical but not pathognomonic of the disease, with most cases of primary CNS lymphoma involving the corpus callosum, periventricular white matter, thalamus, or basal ganglia (Fig 33c, 33d). Expansile or tumefactive lesions of the corpus callosum are usually either infiltrating glial neoplasms or primary CNS lymphoma, which is also an infiltrating process (Fig 33c, 33d) (42,55–58). Primary CNS lymphoma is usually intraaxial, whereas meningeal involvement (dural, arachnoid, and pial) is most often secondary (metastatic) to the CNS (57,58). Primary CNS lymphomas appear hyperattenuating on non–contrast-enhanced CT scans and have a homogeneous “lamb’s wool” appearance on contrast-enhanced images (Fig 33a, 33b). Heterogeneity or ring enhancement is more

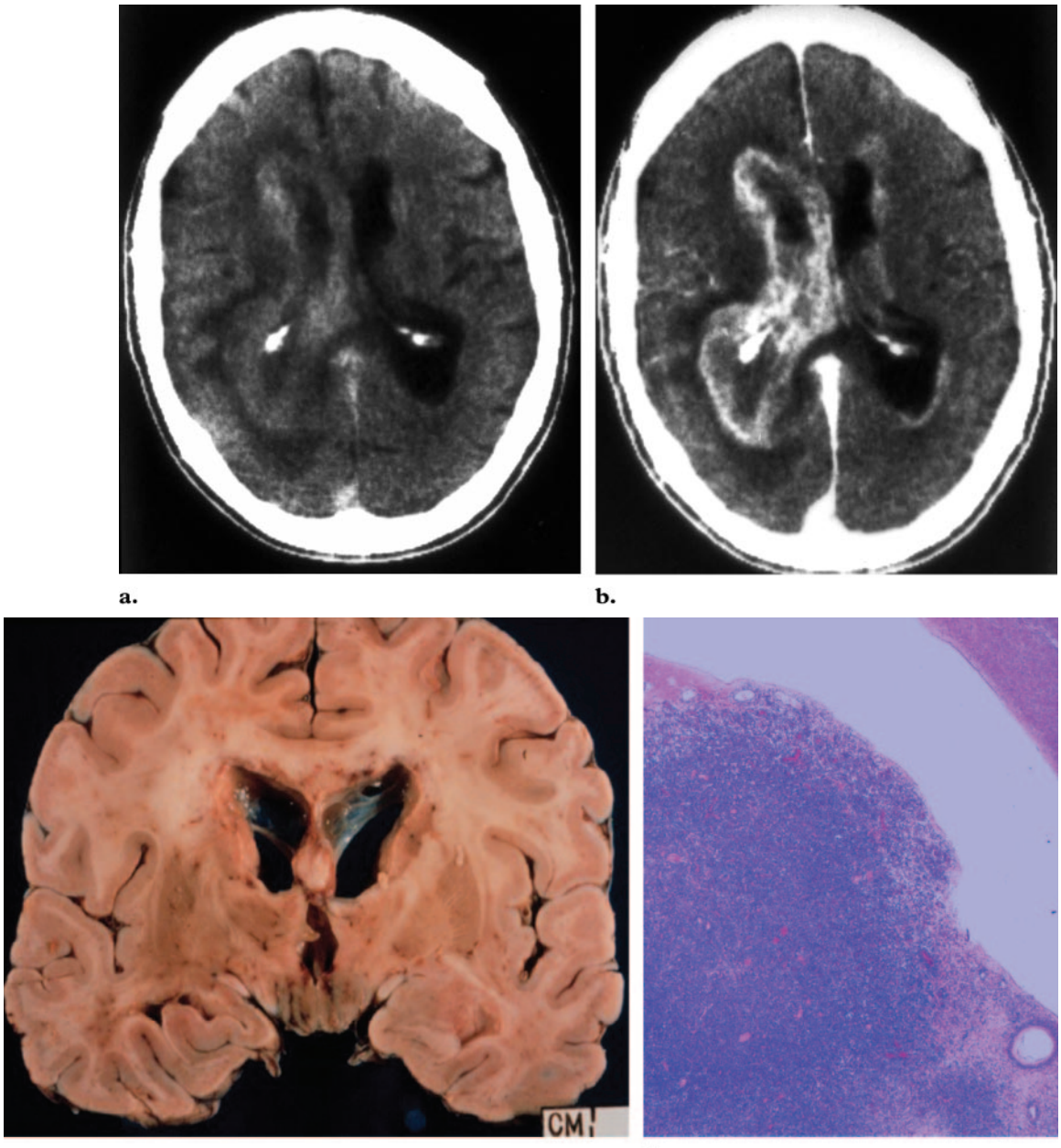

Figure 33. Thick periventricular enhancement in primary CNS lymphoma in an adult patient with AIDS. **(a)** Axial nonenhanced CT scan shows a thick rind of periventricular hyperattenuation, with surrounding vasogenic edema. **(b)** Axial contrast-enhanced CT scan shows abnormal enhancement around both lateral ventricles. This "rind" is much thicker around the right lateral ventricle and involves the same areas that were hyperattenuating before contrast material administration. **(c)** Photograph of a coronally sectioned gross specimen shows periventricular discoloration around the frontal horns, due to neoplastic lymphocyte infiltration. **(d)** Photomicrograph (original magnification, ×250; H-E stain) shows infiltration of small, round, blue cells in the periventricular region, adjacent to the frontal horn of the lateral ventricle.

common in patients with AIDS or other causes of immunosuppression. The lesions appear hypo- or isointense on T1-weighted images and iso- to hyperintense on T2-weighted MR images.

Thin (<2 mm, more often 1 mm) linear enhancement along the margins of the ventricles on CT and MR images is characteristic of infectious ependymitis. Ependymitis and ventriculitis may cause thin linear enhancement along the ventricular (inferior) surface of the corpus callosum. In

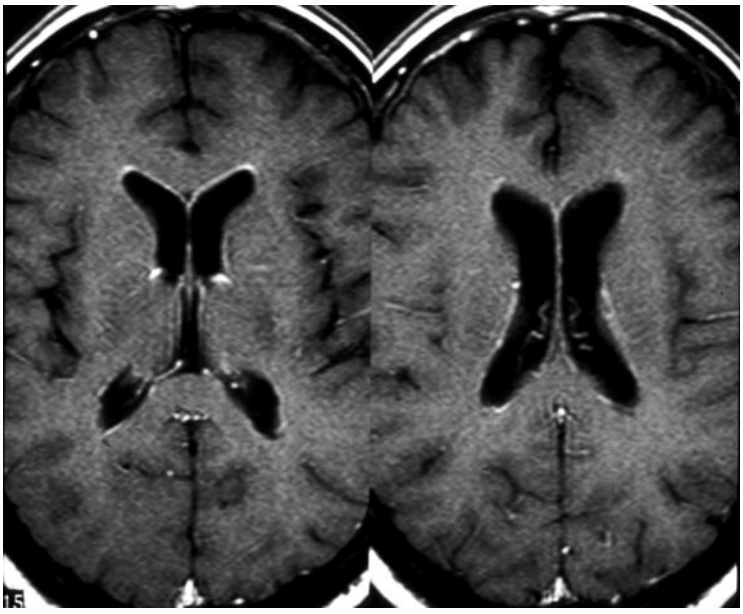

Figure 34. Thin periventricular enhancement in cytomegalovirus ependymitis. Two axial gadolinium-enhanced T1-weighted MR images show abnormal enhancement completely surrounding both lateral ventricles. The enhancement is thin and very uniform. Cytomegalovirus causes an inflammation of the ventricular lining and produces ependymitis. (Courtesy of Vince Mathews, MD, University of Indiana, Indianapolis, Ind.)

immunocompromised patients, this finding might signal an infection (ventriculitis) caused by cytomegalovirus (Fig 34). Cytomegalovirus is a member of the herpes family of viruses. Patients with ventricular shunt catheters may also develop ventriculitis from an ascending infection in the shunt tubing.

References

1. Sage MR, Wilson AJ, Scroop R. Contrast media and the brain: the basis of CT and MR imaging enhancement. Neuroimaging Clin N Am 1998;8:695–707.
2. Provenzale JM, Mukundan S, Dewhirst M. The role of blood-brain barrier permeability in brain tumor imaging and therapeutics. AJR Am J Roentgenol 2005;185:763–767.
3. Wilms G, Demaerel P, Bosmans H, Marchal G. MRI of non-ischemic vascular disease: aneurysms and vascular malformations. Eur Radiol 1999;9:1055–1060.
4. Meltzer CC, Fukui MB, Kanal E, Smirniotopoulos JG. MR imaging of the meninges. I. Normal anatomic features and nonneoplastic disease. Radiology 1996;201:297–308.
5. Burke JW, Podrasky AE, Bradley WG Jr. Meninges: benign postoperative enhancement on MR images. Radiology 1990;174:99–102.
6. Mittl RL Jr, Yousem DM. Frequency of unexplained meningeal enhancement in the brain after lumbar puncture. AJNR Am J Neuroradiol 1994;15:633–638.
7. Phillips ME, Ryals TJ, Kambhu SA, Yuh WT. Neoplastic vs inflammatory meningeal enhancement with Gd-DTPA. J Comput Assist Tomogr 1990;14:536–541.
8. Paldino M, Mogilner AY, Tenner MS. Intracranial hypotension syndrome: a comprehensive review. Neurosurg Focus 2003;15:1–8.
9. Buetow MP, Buetow PC, Smirniotopoulos JG. Typical, atypical, and misleading features in meningioma. RadioGraphics 1991;11:1087–1106.
10. Sheporaitis LA, Osborn AG, Smirniotopoulos JG, Clunie DA, Howieson J, D'Agostino AN. Radiologic-pathologic correlation: intracranial meningioma. AJNR Am J Neuroradiol 1992;13:29–37.
11. Elster AD, Challa VR, Gilbert TH, Richardson DN, Contento JC. Meningiomas: MR and histopathologic features. Radiology 1989;170:857–862.
12. New PF, Aronow S, Hesselink JR. National Cancer Institute study: evaluation of computed tomography in the diagnosis of intracranial neoplasms—IV. Meningiomas. Radiology 1980;136:665–675.
13. Aoki S, Sasaki Y, Machida T, Tanioka H. Contrast-enhanced MR images in patients with meningioma: importance of enhancement of the dura adjacent to the tumor. AJNR Am J Neuroradiol 1990;11:935–938.
14. Gupta S, Gupta RK, Banerjee D, Gujral RB. Problems with the dural tail sign. Neuroradiology 1993;35:541–542.
15. Tien RD, Yang PJ, Chu PK. Dural tail sign: a specific MR sign for meningioma? J Comput Assist Tomogr 1991;15:64–66.
16. Nakau H, Miyazawa T, Tamai S, et al. Pathologic significance of meningeal enhancement ("flare sign") of meningiomas on MRI. Surg Neurol 1997;48:584–590.

17. Nagele T, Petersen D, Klose U, Grodd W, Opitz H, Voigt K. The dural tail adjacent to meningiomas studied by dynamic contrast-enhanced MRI: a comparison with histopathology. Neuroradiology 1994;36:303–307.
18. Spellerberg B, Prasad S, Cabellos C, Burroughs M, Cahill P, Tuomanen E. Penetration of the blood-brain barrier: enhancement of drug delivery and imaging by bacterial glycopeptides. J Exp Med 1995;182:1037–1043.
19. Schaefer PW. Diffusion-weighted imaging as a problem-solving tool in the evaluation of patients with acute strokelike syndromes. Top Magn Reson Imaging 2000;11:300–309.
20. Provenzale JM, Petrella JR, Cruz LC Jr, Wong JC, Engelter S, Barboriak DP. Quantitative assessment of diffusion abnormalities in posterior reversible encephalopathy syndrome. AJNR Am J Neuroradiol 2001;22:1455–1461.
21. Silverstein AM, Alexander JA. Acute postictal cerebral imaging. AJNR Am J Neuroradiol 1998;19: 1485–1488.
22. Burke JW, Mathews VP, Elster AD, Ulmer JL, McLean FM, Davis SB. Contrast-enhanced magnetization transfer saturation imaging improves MR detection of herpes simplex encephalitis. AJNR Am J Neuroradiol 1996;17:773–776.
23. Davis JM, Davis KR, Kleinman GM, Kirchner HS, Taveras JM. Computed tomography of herpes simplex encephalitis, with clinicopathological correlation. Radiology 1978;129:409–417.
24. Zimmerman RD, Russell EJ, Leeds NE, Kaufman D. CT in the early diagnosis of herpes simplex encephalitis. AJR Am J Roentgenol 1980; 134:61–66.
25. Kinkel WR, Jacobs L, Kinkel PR. Gray matter enhancement: a computerized tomographic sign of cerebral hypoxia. Neurology 1980;30:810–819.
26. Ketonen L, Koskiniemi ML. Computed tomography appearance of herpes simplex encephalitis. Clin Radiol 1980;31:161–165.
27. Muller JP, Destee A, Lozes G, Pruvo JP, Jomin M, Warot P. Transient cortical contrast enhancement on CT scan in migraine. Headache 1987;27:578–579.
28. Enzmann DR, Ranson B, Norman D, Talberth E. Computed tomography of herpes simplex encephalitis. Radiology 1978;129:419–425.
29. Elster AD, Moody DM. Early cerebral infarction: gadopentetate dimeglumine enhancement. Radiology 1990;177:627–632.
30. Crain MR, Yuh WT, Greene GM, et al. Cerebral ischemia: evaluation with contrast-enhanced MR imaging. AJNR Am J Neuroradiol 1991;12:631–639.
31. Inoue Y, Takemoto K, Miyamoto T, et al. Sequential computed tomography scans in acute cerebral infarction. Radiology 1980;135:655–662.
32. Runge VM, Kirsch JE, Wells JW, Dunworth JN, Woolfolk CE. Visualization of blood-brain barrier disruption on MR images of cats with acute cerebral infarction: value of administering a high dose of contrast material. AJR Am J Roentgenol 1994; 162:431–435.
33. Norton GA, Kishore PR, Lin J. CT contrast enhancement in cerebral infarction. AJR Am J Roentgenol 1978;131:881–885.
34. Stark AM, Tscheslog H, Buhl R, Held-Feindt J, Mehdorn HM. Surgical treatment for brain metastases: prognostic factors and survival in 177 patients. Neurosurg Rev 2005;28:115–119.
35. Pedersen H, McConnell J, Harwood-Nash DC, Fitz CR, Chuang SH. Computed tomography in intracranial, supratentorial metastases in children. Neuroradiology 1989;31:19–23.
36. Schwartz KM, Erickson BJ, Lucchinetti C. Pattern of T2 hypointensity associated with ring-enhancing brain lesions can help to differentiate pathology. Neuroradiology 2006;48:143–149.

37. Brant-Zawadzki M, Enzmann DR, Placone RC Jr, et al. NMR imaging of experimental brain abscess: comparison with CT. AJNR Am J Neuroradiol 1983;4:250–253.
38. Britt RH, Enzmann DR, Placone RC Jr, Obana WG, Yeager AS. Experimental anaerobic brain abscess. J Neurosurg 1984;60:1148–1159.
39. Britt RH, Enzmann DR, Yeager AS. Neuropathological and computerized tomographic findings in experimental brain abscess. J Neurosurg 1981;55:590–603.
40. Haimes AB, Zimmerman RD, Morgello S, et al. MR imaging of brain abscesses. AJR Am J Roentgenol 1989;152:1073–1085.
41. Daumas-Duport C, Scheithauer BW, O'Fallon J, Kelly P. Grading of astrocytomas: a simple and reproducible method. Cancer 1988;62:2152–2165.
42. Rees JH, Smirniotopoulos JG, Jones RV, Wong K. Glioblastoma multiforme: radiologic-pathologic correlation. RadioGraphics 1996;16:1413–1438.
43. Rong Y, Durden DL, Van Meir EG, Brat DJ. 'Pseudopalisading' necrosis in glioblastoma: a familiar morphologic feature that links vascular pathology, hypoxia, and angiogenesis. J Neuropathol Exp Neurol 2006;65:529–539.
44. Machein MR, Plate KH. VEGF in brain tumors. J Neurooncol 2000;50:109–120.
45. Takano S, Kamiyama H, Tsuboi K, Matsumura A. Angiogenesis and antiangiogenic therapy for malignant gliomas. Brain Tumor Pathol 2004;21:69–73.
46. Fulham MJ, Melisi JW, Nishimiya J, Dwyer AJ, Di CG. Neuroimaging of juvenile pilocytic astrocytomas: an enigma. Radiology 1993;189:221–225.
47. Takeuchi H, Kubota T, Sato K, Arishima H. Ultrastructure of capillary endothelium in pilocytic astrocytomas. Brain Tumor Pathol 2004;21:23–26.
48. Ho VB, Smirniotopoulos JG, Murphy FM, Rushing EJ. Radiologic-pathologic correlation: hemangioblastoma. AJNR Am J Neuroradiol 1992;13:1343–1352.
49. Beni-Adani L, Gomori M, Spektor S, Constantini S. Cyst wall enhancement in pilocytic astrocytoma: neoplastic or reactive phenomena. Pediatr Neurosurg 2000;32:234–239.
50. Cotton F, Weiner HL, Jolesz FA, Guttmann CR. MRI contrast uptake in new lesions in relapsing-remitting MS followed at weekly intervals. Neurology 2003;60:640–646.
51. Cha S, Knopp EA, Johnson G, Wetzel SG, Litt AW, Zagzag D. Intracranial mass lesions: dynamic contrast-enhanced susceptibility-weighted echo-planar perfusion MR imaging. Radiology 2002;223:11–29.
52. Masdeu JC, Moreira J, Trasi S, Visintainer P, Cavaliere R, Grundman M. The open ring: a new imaging sign in demyelinating disease. J Neuroimaging 1996;6:104–107.
53. Masdeu JC, Quinto C, Olivera C, Tenner M, Leslie D, Visintainer P. Open-ring imaging sign: highly specific for atypical brain demyelination. Neurology 2000;54:1427–1433.
54. Bot JC, Barkhof F, Nijeholt G, et al. Differentiation of multiple sclerosis from other inflammatory disorders and cerebrovascular disease: value of spinal MR imaging. Radiology 2002;223:46–56.
55. Reinarz SJ, Coffman CE, Smoker WR, Godersky JC. MR imaging of the corpus callosum: normal and pathologic findings and correlation with CT. AJR Am J Roentgenol 1988;151:791–798.
56. Ciricillo SF, Rosenblum ML. Use of CT and MR imaging to distinguish intracranial lesions and to define the need for biopsy in AIDS patients. J Neurosurg 1990;73:720–724.
57. Tomlinson FH, Kurtin PJ, Suman VJ, et al. Primary intracerebral malignant lymphoma: a clinicopathological study of 89 patients. J Neurosurg 1995;82:558–566.
58. Koeller KK, Smirniotopoulos JG, Jones RV. Primary central nervous system lymphoma: radiologic-pathologic correlation. RadioGraphics 1997;17:1497–1526.

This article meets the criteria for 1.0 credit hour in category 1 of the AMA Physician's Recognition Award. To obtain credit, see accompanying test at http://www.rsna.org/education/rg_cme.html.

From the Archives of the AFIP : Patterns of Contrast Enhancement in the Brain and Meninges

James G. Smirniotopoulos, MD et al

RadioGraphics 2007; 27:525–551 • **Published online** 10.1148/rg.272065155 • **Content Code:** NR

Page 526
Contrast material enhancement in the central nervous system (CNS) is a combination of two primary processes: intravascular (vascular) enhancement and interstitial (extravascular) enhancement (1,2).

Page 528
Intracranial hypotension is a benign cause of pachymeningeal enhancement that may be localized or diffuse and can be seen on MR images in patients after surgery or with idiopathic loss of cerebrospinal fluid pressure.

Page 530
However, later studies helped confirm that most of the linear dural enhancement, especially when it was more than a centimeter away from the tumor bulk, was probably caused by a reactive process (17). This reactive process includes both vasocongestion and accumulation of interstitial edema, both of which increase the thickness of the dura mater.

Page 533
Superficial enhancement of the brain parenchyma is usually caused by vascular or inflammatory processes and is only rarely neoplastic.

Page 541
The rim of reactive tissue is usually thin (2–7 mm), uniformly convex, and smooth on both the outer and inner aspects.

Page 543
Imaging features of a necrotic neoplasm include a thick irregular ring with a shaggy inner margin, multilocular and complex ring patterns, and a wall that is thicker than 10 mm (at least in some areas).

Page 545
Fluid-secreting neoplasms may, therefore, demonstrate an incomplete ring of enhancement, because part of the margin surrounding the fluid is neoplastic and part is nonneoplastic (compressed or gliotic brain tissue). Occasionally, thin (<2-mm) rim enhancement, representing gliosis and not neoplastic tissue, can be seen in a pilocytic astrocytoma.